

1 **Development and testing of scenarios for implementing land use and land cover changes during**
2 **the Holocene in Earth System Model Experiments**

3
4 Sandy P. Harrison¹, Marie-José Gaillard², Benjamin D. Stocker^{3,4}, Marc Vander Linden⁵, Kees Klein
5 Goldewijk^{6,7}, Oliver Boles⁸, Pascale Braconnot⁹, Andria Dawson¹⁰, Etienne Fluet-Chouinard¹¹, Jed
6 O. Kaplan^{12,13}, Thomas Kastner¹⁴, Francesco S.R. Pausata¹⁵, Erick Robinson¹⁶, Nicki J.
7 Whitehouse¹⁷, Marco Madella^{18,19,20}, Kathleen D. Morrison⁸

8
9 Ms for Geoscientific Model Development (PMIP special issue)

10
11 1: Department of Geography and Environmental Science, University of Reading, Reading, UK

12 2: Department of Biology and Environmental Science, Linnaeus University, Kalmar, Sweden

13 3: Ecological and Forestry Applications Research Centre, Cerdanyola del Vallès, Spain

14 4: Department of Earth System Science, Stanford University, Stanford, CA 94305, USA

15 5: Department of Archaeology, University of Cambridge, UK

16 6: PBL Netherlands Environmental Assessment Agency, The Hague, The Netherlands

17 7: Copernicus Institute of Sustainable Development, Utrecht University, The Netherlands

18 8: University Museum of Archaeology & Anthropology, University of Pennsylvania, Philadelphia,
19 USA

20 9: Laboratoire des Sciences du Climat et de l'Environnement, Gif-sur-Yvette, France

21 10: Department of General Education, Mount Royal University, Calgary, Canada

22 11: Department of Earth System Science, Stanford University, California, USA

23 12: Department of Earth Sciences, University of Hong Kong, Hong Kong

24 13: Institute of Geography, University of Augsburg, Augsburg, Germany

25 14: Senckenberg Biodiversity and Climate Research Centre, Frankfurt am Main, Germany

26 15: Centre ESCER, Department of Earth and Atmospheric Sciences, University of Quebec in
27 Montreal, Montreal, Canada

28 16: Department of Anthropology, University of Wyoming, Laramie, Wyoming, USA

29 17: School of Geography, Earth and Environmental Science, University of Plymouth, Plymouth,
30 UK

31 18: Department of Humanities (CaSEs), University Pompeu Fabra, Barcelona, Spain

32 19: ICREA Passeig Lluís Companys 23 08010 Barcelona, Spain

33 20: School of Geography, Archaeology and Environmental Studies, University of Witwatersrand,
34 Johannesburg, South Africa

35 **Abstract:** Anthropogenic changes in land use and land cover (LULC) during the pre-industrial
36 Holocene could have affected regional and global climate. Existing scenarios of LULC changes
37 during the Holocene are based on relatively simple assumptions and highly uncertain estimates of
38 population changes through time. Archaeological and palaeoenvironmental reconstructions have the
39 potential to refine these assumptions and estimates. The Past Global Changes (PAGES) LandCover6k
40 initiative is working towards improved reconstructions of LULC globally. In this paper, we document
41 the types of archaeological data that are being collated and how they will be used to improve LULC
42 reconstructions. Given the large methodological uncertainties involved, both in reconstructing LULC
43 from the archaeological data and in implementing these reconstructions into global scenarios of
44 LULC, we propose a protocol to evaluate the revised scenarios using independent pollen-based
45 reconstructions of land cover and climate. Further evaluation of the revised scenarios involves
46 carbon-cycle model simulations to determine whether the LULC reconstructions are consistent with
47 constraints provided by ice-core records of CO₂ evolution and modern-day LULC. Finally, the
48 protocol outlines how the improved LULC reconstructions will be used in palaeoclimate simulations
49 in the Palaeoclimate Modelling Intercomparison Project to quantify the magnitude of anthropogenic
50 impacts on climate through time and ultimately to improve the realism of Holocene climate
51 simulations.

52

1 Introduction and Motivation

Today, ca 10% the ice-free land surface is estimated to be intensively managed and much of the remainder is under less intense anthropogenic use or influenced by human activities (Arneeth et al., 2019). Substantial transformations of natural ecosystems by humans began with the geographically diachronous shift from hunting and gathering characteristic of the Mesolithic to cultivation and more permanent settlement during the Neolithic period (Mazoyer and Roudart, 2006; Zohary et al., 2012; Tauger, 2013; Maezumi et al. 2018), although there is controversy about the relative importance of climate changes and human impact on landscape development both during and since that time. Resolving the uncertainty about the extent and timing of land use is important because changes in land cover as a result of land use (land use land cover: LULC) have the potential to impact climate and the carbon cycle. Direct climate impacts occur through changes in the surface-energy budget resulting from modifications of surface albedo, evapotranspiration, and canopy structure (biophysical impacts, e.g. Pongratz et al., 2010; Myhre et al., 2013; Perugini et al., 2017). LULC affects the carbon cycle through modifications in vegetation and soil carbon storage (biogeochemical impacts, e.g. Pongratz et al., 2010; Mahowald et al., 2017) and turnover times, which changes the C sink/source capacity of the terrestrial biosphere. LULC changes have contributed substantially to the increase in atmospheric greenhouse gases during the industrial period (Le Quéré et al., 2018). It has been suggested that greenhouse gas emissions associated with Neolithic LULC changes were sufficiently large to offset climate cooling after the Mid-Holocene (the overdue-glaciation hypothesis: Ruddiman 2003). Although this has been challenged for several reasons, including inconsistency with the land carbon balance derived from ice-core and peat records (e.g. Joos et al., 2004; Kaplan et al., 2011; Singarayer et al., 2011; Mitchell et al., 2013; Stocker et al. 2017), a LULC impact on climate in more recent millennia appears more plausible.

Climate model simulations have shown that LULC changes have discernible impacts on climate, both in regions with large prescribed changes in LULC and in teleconnected regions with no major local human activity (Vavrus et al., 2008; Pongratz et al., 2010; He et al., 2014; Smith et al., 2016). At the global scale, the biogeophysical effects of the accumulated LULC change during the Holocene which resulted in reconstructed land cover patterns in 1850CE have been estimated to cause a slight cooling (0.17 °C) that is offset by the biogeochemical warming (0.9 °C), giving a net global warming (0.73 °C) (He et al., 2014). However, in these simulations, biophysical and biogeochemical effects were of comparable magnitude in the most intensively altered landscapes of Europe, Asia, and North America (He et al., 2014). Using parallel simulations, with and without LULC changes, Smith et al. (2016) showed that detectable temperature changes due to LULC could have occurred as early as 7000 years ago (7ka BP) in summer and throughout the year by 3ka BP. All of these conclusions, however, are obviously contingent on the imposed LULC forcing, which is highly uncertain.

There have been several attempts to map LULC changes through time (e.g. Ramankutty and Foley, 1999; Pongratz et al., 2008; Kaplan et al., 2011; Klein Goldewijk et al. 2011; Klein Goldewijk et al. 2017a, b). All of these reconstructions assume that anthropogenic land use is a function of population density and the suitability of land for crops and/or pasture. They then use estimates of regional population trends through time in combination with assumptions about per-capita land use and spatial land use allocation schemes to estimate anthropogenic changes in LULC across time and space. However, differences in the underlying assumptions about land-use per capita, which are generalized from limited and often site-specific data, have resulted in large differences in the final reconstructions (Gaillard et al., 2010; Kaplan et al., 2017). Hence, there are still very large uncertainties about the timing and magnitude of LULC changes, both at a global and at a regional scale (Figure 1).

There is a wealth of archaeological, historical and palaeo-vegetation data that could be used to

103 improve the relatively simple rules used to generate global LULC reconstructions. For example,
104 settlement density and numbers of radiocarbon-dated artifacts can be used to infer population sizes
105 and their temporal dynamics (Rick, 1987; Williams, 2012; Silva and Vander Linden, 2017).
106 Carbonised and waterlogged plant remains and animal bones can be used to infer the nature of
107 agriculture at a site, although their presence provides no quantitative information about the area under
108 cultivation (Wright, 2003; Lyman 2008; Orton et al., 2016). Although the record of LULC is likely
109 to be patchy and incomplete, because of preservation and sampling issues, systematic use of
110 archaeological data is one important way to improve current LULC scenarios.

111
112 The Past Global Change (PAGES, <http://www.pastglobalchanges.org/>) LandCover6k Working
113 Group (<http://pastglobalchanges.org/ini/wg/landcover6k>) is currently working to develop a rigorous
114 and robust approach to provide data and data products that can be used to inform reconstructions of
115 LULC (Gaillard et al., 2018). LULC changes are taken into account in simulations currently being
116 made in the current phase of the Coupled Model Intercomparison Project (CMIP6) for the historic
117 period and the future scenario runs (Eyring et al., 2016). They are also included in simulations of the
118 past millennium (Jungclauss et al., 2017), in order to ensure that these runs mesh seamlessly with the
119 historic simulations. However, the Land Use Harmonisation data set (LUH2: Hurtt et al., 2017) only
120 extend back to 850 CE and thus LULC changes are currently not included in the CMIP6 palaeoclimate
121 simulations, including mid-Holocene simulations, that are used as a test of how well state-of-the-art
122 climate models reproduce large climate changes. In this paper, we discuss how archaeological data
123 will be used to improve global LULC reconstructions for the Holocene. Given that there are large
124 uncertainties associated with the primary data and further uncertainties may be introduced when this
125 information is used to modify existing LULC scenarios, we outline a series of tests that will be used
126 to evaluate whether the revised scenarios are consistent with the changes implied by independent
127 pollen-based reconstructions of land cover and whether they produce more realistic estimates of both
128 carbon cycle and climate change. Finally, we present a protocol for implementing LULC in Earth
129 System Model simulations to be carried out in the current phase of the Palaeoclimate Modelling
130 Intercomparison Project (PMIP: Otto-Bleisner et al., 2017; Kageyama et al., 2018). However, the
131 data sets and protocol will also be useful in later phases of other CMIP projects, including the Land
132 Use Model Intercomparison Project (LUMIP) and the Land Surface, Snow and Soil Moisture Model
133 Intercomparison Project (LS3MIP) (Lawrence et al., 2016; van den Hurk et al., 2016).

134
135

136 **2 LandCover6k Methodology**

137

138 The primary source of information about human exploitation of the landscape comes from
139 archaeological data. In general, these data are site specific and spatiotemporal coverage is often
140 patchy, and the types and quality of evidence available vary between sites and regions. Generalising
141 from site-specific data to landscape or regional scales involves making assumptions about human
142 behaviour and cultural practices. Because of the inherent uncertainties, we advocate an iterative
143 approach to incorporate archaeological data into LULC scenarios in LandCover6k (Fig. 2). We
144 propose to revise the LULC scenario by incorporation of diverse archaeological inputs (Fig. 2, phase
145 1; see Sections 3 and 4) and to test the revised LULC scenarios for their plausibility and consistency
146 with other lines of evidence (Fig. 2, phase 2 with iterative testing; see Sections 5-7). As a first test,
147 the revised LULC scenarios of the extent of cropland and grazing land through time will be compared
148 with independent data on land-cover changes, specifically pollen-based reconstructions of the extent
149 of open land (see e.g. Trondman et al., 2015; Kaplan et al., 2017) (Section 5). Further testing the
150 LULC scenarios involve sensitivity tests using global climate models (Section 6) and global
151 vegetation-carbon cycle models (Section 7). While the computational cost of the climate simulations
152 can be minimized using equilibrium time-slice simulations, the carbon cycle constraint relies on

153 transient simulations, but may be derived from uncoupled, land-only simulations. Simulated climates
154 at key times can be evaluated against reconstructions of climate variables (e.g. Bartlein et al., 2011)
155 (Section 6). The parallel evolution of CO₂ and its isotopic composition ($\delta^{13}\text{C}$) can be used to derive
156 the carbon balance of the terrestrial biosphere and the ocean separately (Elsig et al., 2009) and, in
157 combination with estimates for other contributors to land carbon changes such as C sequestration by
158 peat buildup, provides a strong constraint on the evolution of LULC through time. An under- or over-
159 prediction of anthropogenic LULC-related CO₂ emissions during a specific interval results in
160 consequences for the dynamics of the atmospheric greenhouse gas burden in subsequent times
161 (Stocker et al., 2017) (Section 7). Thus, these tests can be used to identify issues in the original
162 archaeological datasets and/or the way these data were incorporated into the LULC scenarios that
163 require further refinement. Phase 3 of the protocol (Fig. 2) proposes specific implementation of the
164 revised LULC in Earth System Model simulations (Section 8).

165

166 **3 Archaeological data inputs**

167

168 LandCover6k is creating a number of products that will be used to improve the LULC scenarios
169 (Figure 2). Here, we summarise the important features of these data products before showing how
170 they will be incorporated within a scenario-development framework.

171

172 **3.1 Population dynamics from ¹⁴C data**

173 Radiocarbon is the most routinely used absolute dating technique in archaeology, especially for the
174 Holocene. Many thousands of radiocarbon dates are available from the archaeological literature. A
175 number of regional and pan-regional initiatives are compiling these records through exhaustive
176 survey of the archaeological literature (e.g. the Canadian Archaeological Radiocarbon Database:
177 <https://www.canadianarchaeology.ca/>). Statistical approaches, such as summed probability
178 distributions (SPDs), can then be used to infer past demographic fluctuations from these compilations
179 (Figure 3). This method assumes that the more people there were, the more remains of their various
180 activities they left behind, and that this is directly reflected in the number of samples excavated and
181 dated (Rick, 1987; Robinson et al., 2019). There are biases that could affect the expected one-to-one
182 relationship between number of people and number of radiocarbon dates on archaeological material,
183 including lack of uniform sampling through time and space caused by different archaeological
184 research interests and traditions in different regions and increased preservation issues with increasing
185 age, but these can be minimised through auditing the datasets. Assessment of the robustness of
186 population reconstructions through time can be made statistically, by comparing a null hypothesis of
187 demographic growth constructed from an exponential fit to the data with the actual record of number
188 of dates through time (Shennan et al., 2013; Timpson et al., 2014). Mathematical simulations show
189 that the method is relatively robust for large sample sizes (Williams, 2012). Radiocarbon dates have
190 been successfully used in several regions to identify population fluctuations associated with the
191 introduction of farming and subsequent changes in farming regimes (western Europe: Shennan et al.,
192 2013; Wyoming: Zahid et al., 2016; South Korea: Oh et al., 2017; see also Freeman et al., 2018) as
193 well as climatic oscillations (Ireland: Whitehouse et al., 2014; Japan: Crema et al., 2016).

194

195 **3.2 Date of first agriculture**

196 Radiocarbon dates can also be used to track the timing and process of dispersal events, such as the
197 diffusion of plant and animal domesticates from their initial centres of domestication. Since the
198 distribution of samples is often patchy, geostatistical techniques such as kriging and splines are used
199 to spatially interpolate the information in order to provide quantitative estimates of the timing of
200 spread. Work carried out in Europe (Bocquet-Appel et al., 2009), Asia (Silva et al., 2015), and Africa
201 (Russell et al., 2014) demonstrates that there are different rates of diffusion even within a region,
202 reflecting the possible impact of natural features (e.g. waterways, elevation, ecology) on diffusion

203 rates (Davison et al., 2006; Silva and Steele, 2014). Numerous studies provide robust local estimates
204 for the earliest regional occurrence of agriculture and these are being synthesized to provide a global
205 product within LandCover6k (Figure 2).
206

207 **3.3 Global land-use and livestock maps**

208 Maps of the distribution of archaeological sites or of areas linked to a given food production system
209 have been produced for individual site catchments or small regions (e.g. Zimmermann et al., 2009;
210 Barton et al., 2010; Kay et al., in press). LandCover6k is developing global land-use maps for specific
211 time windows, using a global hierarchical classification of land-use categories (Morrison et al., 2018)
212 based on land-use types that are widely recognised from the archaeological record. At the highest
213 level, the maps distinguish between areas where there is no (or only limited) evidence of land use,
214 and areas characterized by hunting/foraging/fishing activities, pastoralism, agriculture, and
215 urban/extractive land use (Fig. 4). Except in the cases where land use is minimal (no human land use,
216 extensive/minimal land use), further distinctions are subsequently made to encompass the diversity
217 of land-use activities in each land-use type (Fig. 4). A third level of distinction is made in the case of
218 two categories (agroforestry, wet cultivation) where there are very different levels of intervention in
219 different regions. Explanations of this terminology are given in Morrison et al. (2018). The
220 LandCover6k land-use maps (see e.g. Fig. 5) will be based on different methods ranging from kernel-
221 density estimates to expert assessments depending on the quality and quantity of the archaeological
222 information available from different regions.
223

224 There is considerable variation in how intensely land is used both for crops and for grazing within
225 broad land-use categories both geographically and through time (Ford and Clarke, 2015; Styring et
226 al., 2017). Maps of land-use types do not provide direct information on the intensity of farming
227 practices or how they translate into per-capita land use. Archaeological data about agricultural yields,
228 combined with information from analogous contemporary cultures, historical information (e.g.
229 Pongratz et al., 2008) and theoretical estimates of land use required to meet dietary and energy
230 requirements (e.g. Hughes et al., 2018), can be used to provide regional estimates of per-capita land
231 use for specific land-use categories. LandCover6k will synthesise this information to allow regionally
232 specific estimates of per-capita land use to be derived from the global land-use maps.
233

234 Information about the extent of grazing land is an important input to LULC scenarios but, from a
235 carbon-cycle modelling perspective, the amount of biomass removed by grazing is also a key
236 parameter. Biomass loss varies not only with population size but also with the type of animal being
237 reared (Herrero et al., 2013; Phelps & Kaplan, 2017) and thus information about what animals were
238 present at a given location and estimates of population sizes are needed for LULC scenarios. Although
239 the conditions of bone preservation vary across the globe due to factors such as soil acidity, animal
240 bones are routinely excavated (Lyman, 2008; Reitz & Wing, 2008). Morphometric analysis of bones,
241 along with collateral information such as age-related culling patterns, make it possible to determine
242 whether these are the remains of domesticated species. We thus have a relatively precise idea of when
243 livestock were introduced into a region and what types of animal were being reared at a given time,
244 and can also make informed estimates of population size. Although the level of detail will vary
245 geographically, this information can be used to produce global livestock maps.
246

247 The harvesting of wood for domestic fires, building, and for industrial activities such as
248 transportation, pottery-making and metallurgy is an important aspect of human exploitation of the
249 landscape in the pre-industrial period (McGrath et al., 2015). It has been argued that even Mesolithic
250 hunter-gatherer communities shaped their environment through wood harvesting (Bishop et al.,
251 2015). Approaches have been developed to quantifying the wood harvest associated with
252 archaeological settlements at specific times based on the evidence of types of wood use, household

253 energy requirements, population size, and calorific value of the wood used (see e.g. Marston, 2009;
254 Janssen et al., 2017). However, quantitative information on ancient technology and lifestyle is sparse
255 and direct estimates of the amount of wood harvest through time are likely to remain highly uncertain
256 (Marston et al., 2017; Veal, 2017). Nevertheless, by combining modelling approaches with improved
257 estimates of population size should allow changes in wood harvesting to be taken into account in
258 LULC scenarios.

259
260

261 **4. Incorporation of archaeological data in LULC scenarios**

262

263 The existing LULC scenarios are substantially dependent on historical regional population estimates
264 at key times, which are then linearly interpolated to provide a year-by-year estimate of population.
265 Estimates of regional population growth based on suitably-screened ¹⁴C data can be used to modify
266 existing population growth curves (Figure 6), both in terms of establishing the initial date of human
267 presence and by modifying a linear growth curve to allow for intervals of population growth and
268 decline.

269

270 Information on the timing of the first appearance of agriculture at specific locations can be used to
271 constrain the temporal record of LULC changes in the scenarios. This information can also be used
272 to allocate LULC changes geographically across regions (Figure 6). Global land-use maps can be
273 used to identify areas where there was no permanent agricultural activity at a given time (e.g. either
274 unsettled areas or areas occupied by hunter-gatherer communities) and provide a further constraint
275 on the geographic extent of LULC changes (Figure 6). The type of agriculture, including whether the
276 region was predominantly used for tree or annual crops or for pasture, modifies the area of open land
277 specified in the scenarios. Information on the extent of rain-fed versus irrigated agriculture, as
278 indicated by the presence of irrigation structures associated with archaeological sites, can also be used
279 to refine the distribution of these classes in the LULC scenarios. Per-capita land-use estimates and
280 their changes through time (see e.g. Hughes et al., 2018; Weiberg et al., 2019) provide a further
281 refinement of the LULC scenarios, allowing a better characterization of the distinction between e.g.
282 areas given over to extensive versus intensive animal production (rangeland versus pasture in the
283 HYDE 3.2 terminology). There will remain areas of the world for which this kind of fine-grained
284 information is not available. Nevertheless, by incorporating information where this exists, the
285 LandCover6k products will contribute to a systematic refinement of LULC scenarios. Iterative testing
286 of the revised scenarios will ensure that they are robust.

287

288

289 **5. Using pollen-based reconstructions of land cover changes to evaluate LULC scenarios**

290

291 Pollen-based vegetation reconstructions can be used to corroborate archaeological information on the
292 date of first agriculture from the appearance of cereals and agricultural weeds. These reconstructions
293 can also be used to test the LULC reconstructions, either using relative changes in forest cover or
294 reconstructions of the area occupied by different land cover types. LandCover6k uses the REVEALS
295 model (Sugita, 2007) to estimate vegetation cover from fossil pollen assemblages. The REVEALS
296 model predicts the relationship between pollen deposition in large lakes and the abundance of
297 individual plant taxa in the surrounding vegetation at a large spatial scale (ca. 100 km x 100 km;
298 Hellman et al., 2008a, b) using models of pollen dispersal and deposition. REVEALS can also be
299 used with pollen records from multiple small lakes or peat bogs (Trondman et al., 2016) although this
300 results in larger uncertainties in the estimated area occupied by individual taxa. The estimates
301 obtained for individual taxa are summed to produce estimates of the area occupied by either plant

302 functional (e.g. summer-green trees, evergreen trees) or land cover (e.g. open land, grazing land,
303 cropland) types.

304
305 The geographic distribution of pollen records is uneven. There are also many areas of the world where
306 environments that preserve pollen (i.e. lakes, bogs, forest hollows) are sparse. Site-based
307 reconstructions of land cover are therefore interpolated statistically to produce spatially continuous
308 reconstructions (Nielsen et al., 2012; Pirzamanbein et al., 2014; Pirzamanbein et al., 2018).
309 LandCover6k uses a 1° resolution grid and all available pollen records in each grid cell to produce an
310 estimate of land cover per grid cell through time. The more pollen records per grid cell and pollen
311 counts per time window, the smaller the estimated error on the land-cover reconstruction. The
312 uncertainties on the pollen-based REVEALS estimates are partly expressed by their standard errors
313 (SEs). These SEs take into account the SE on the relative pollen productivity (RPP) of each plant
314 taxon included in the REVEALS reconstruction and the variability between the site-specific
315 REVEALS estimates (e.g. Trondman et al., 2015). These uncertainties on the pollen-based land cover
316 are considered when these reconstructions are compared with LULC scenarios (Kaplan et al., 2017).
317

318 The REVEALS approach has already been used to produce gridded reconstructions of changes in the
319 amount of open land through time across the northern extratropics (Figure 7; Dawson et al., 2018)
320 These reconstructions provide mean plant cover for time slices of 500 years through the Holocene
321 until 0.7ka BP, and three historical time windows (modern–0.1ka BP, 0.1–0.35ka BP, and 0.35–0.7ka
322 BP). The more pollen samples per time intervals and pollen records per grid cells, the more years
323 within the 500 yrs time slice will be represented in the reconstruction. This implies that the number
324 of years represented in a time-slice reconstruction varies in space and time.

325
326 A major limitation in applying REVEALS globally is requirement for information about the relative
327 pollen productivity (RPP) of individual pollen taxa, which is currently largely lacking for the tropics.
328 However, LandCover6k has been collecting RPPs for China, South-East India, Cameroon, Brazil and
329 Argentina and pollen-based land-cover reconstructions will be available for at sufficient parts of the
330 tropics to allow testing of the scenarios. Another limitation of REVEALS reconstructions is that RPP
331 estimates are available for cultivated cereals but not for other cultivars or cropland weeds, so the
332 LandCover6k reconstructions will generally underestimate cropland cover (Trondman et al., 2015).
333 It may also be possible to use alternative pollen-based reconstructions of land cover changes, such as
334 the Modern Analogue Approach (MAT: e.g. Tarasov et al., 2007; Zanon et al. 2018); pseudo-
335 biomization (e.g. Fyfe et al., 2014) or STEPPS (Dawson et al., 2016). While none of these methods
336 require RPPs, MAT and STEPPS can only be applied in regions where the pollen datasets have dense
337 coverage (such as Europe and North America) and pseudo-biomization is affected by the non-
338 linearity of the pollen-vegetation relationship that the REVEALS approach is designed to remove.
339

340 Comparison of the reconstructions of the extent of open land with the LULC deforestation scenarios
341 will provide a first evaluation of the realism of the revised LULC scenarios (e.g. Kaplan et al., 2017).
342 Underestimation or overestimation of open land in the LULC scenarios is not necessarily an
343 indication that these scenarios are inaccurate because (a) pollen-based reconstructions cannot
344 distinguish between anthropogenic and climatically determined natural open land (e.g. natural
345 grasslands, steppes, wetlands) and (b) REVEALS underestimates cropland cover because there are
346 no RPP estimates for cultivars other than cereals. However, overestimation of the area of open land
347 in the LULC scenarios might suggest problems either in the archaeological inputs or their
348 implementation, especially for times or regions when other evidence indicates cereals were the major
349 crop. In this sense, despite potential problems, the LandCover6k pollen-based reconstructions of land
350 cover will provide an important independent test of the revised LULC scenarios.
351

352 **6. Testing the reliability of improved scenarios using climate-model simulations**

353

354 A second test of the realism of the improved LULC scenarios is to examine whether incorporating
355 LULC changes improves the realism of the simulated climate when compared to palaeoclimate
356 reconstructions (Figure 8). The mid-Holocene (6000 years ago, 6 ka BP) is an ideal candidate for
357 such a test because benchmark data sets of quantitative climate reconstructions are available (e.g.
358 Bartlein et al., 2011), the interval has been a focus through multiple phases of PMIP and control
359 simulations with no LULC have already been run, and evaluation of these simulations has identified
360 regions where there are major discrepancies between simulated and reconstructed climates e.g. the
361 observed expansion of northern hemisphere monsoons, climate changes over Europe, the magnitude
362 of high-latitude warming, and wetter conditions in central Eurasia (Mauri et al., 2014; Harrison et al.,
363 2015; Bartlein et al., 2017). There are discernible anthropogenic impacts on the landscape in many
364 of these regions by 6 ka, although they are not as strong as during the later Holocene and they are not
365 present everywhere. Nevertheless, the 6ka BP interval provides a good focus for testing
366 improvements to the LULC scenarios. Such an evaluation would need to go beyond the global
367 comparison made here (Figure 8) to regional comparisons to identify whether improvements in
368 regions where there is a large anthropogenic impact on land cover do not result in a degradation in
369 the simulated climate elsewhere.

370

371

372 **7. Testing the reliability of improved scenarios using carbon-cycle models**

373

374 Carbon-cycle modelling will be used as a further test of the realism of the improved LULC scenarios.
375 Two constraints are available for testing the realism of past LULC reconstructions. First,
376 reconstructions of LULC history must converge on the present-day state, which is relatively well
377 constrained by satellite land-cover observations and national statistics on the amount of land under
378 use. Reconstructing the extent of past LULC thus reduces to allocating a fixed total amount of land
379 conversion from natural to agricultural use over time. More conversion in earlier periods implies less
380 conversion in later periods. At the continental to global scale, cumulative LULC emissions scale
381 linearly with the agricultural area. LULC scenarios that converge to the present-day state also
382 converge to within a small range of cumulative historical emissions (Stocker et al., 2011; Stocker et
383 al., 2017). Deviations from a linear relationship between extent and emissions are due to differences
384 in biomass density in potential natural and agricultural vegetation of different regions affected by
385 anthropogenic LULC. Differences in cumulative emissions for alternative LULC reconstructions
386 with an identical present-day state are due to the long response time of soil carbon content following
387 a change in carbon inputs and soil cultivation. Conserving the total extent of LULC (and allocating a
388 fixed total expansion over time) is thus approximately equivalent to conserving cumulative historical
389 LULC emissions. Thus, more LULC CO₂ emissions in earlier periods imply less CO₂ emissions in
390 more recent periods.

391

392 The total C budget of the terrestrial biosphere provides a second constraint on LULC emissions
393 through time. The net C balance of the land biosphere, which reflects the sum of all natural and
394 anthropogenic effects on terrestrial C storage, can be reconstructed from ice-core data of past CO₂
395 concentrations and $\delta^{13}\text{C}$ composition (Elsig et al. 2009). Providing that all of the natural contributions
396 to the land C inventory (e.g. the build up of natural peatlands: Loisel et al., 2014) can be specified
397 from independent evidence, the anthropogenic sources can be estimated as the difference between the
398 total terrestrial C budget and natural contributions (Figure 9) at any specific time.

399

400 Transient simulations with a model that simulates CO₂ emissions in response to anthropogenic LULC
401 can be used to test the reliability of the LULC changes through time, by comparing results obtained

402 with prescribed LULC changes through time against a baseline simulation without imposed LULC.
403 This will necessitate making informed decisions about the fraction of land under cultivation that is
404 abandoned or left fallow each year, and the maximum extent of land affected by such episodic
405 cultivation. We envisage using several different offline carbon-cycle models for this purpose in order
406 to take account of uncertainties associated with inter-model differences. The carbon-cycle simulations
407 will be driven by climate outputs (temperature, precipitation and cloud cover) from an existing
408 transient climate simulation made with the ECHAM model (Fischer and Jungclaus, 2011) and CO₂
409 prescribed from ice-core records. The CO₂ emission estimates from these two simulations will then
410 be evaluated using C budget constraints. This evaluation will allow us to pinpoint potential
411 discrepancies between known terrestrial C balance changes and estimated LULC CO₂ emission in
412 given periods over the Holocene.

413

414

415

8. Implementation of LULC in Earth System Model simulations

416

417 We propose a series of simulations to examine the impact of LULC, using the revised LULC scenarios
418 from LandCover6k and building on experiments that are currently being run either in CMIP6-PMIP4
419 (*midHolocene*, *past1000*) or within PMIP although not formally included as CMIP6-PMIP4
420 experiments.

421

422 The *mid-Holocene* (and its corresponding *piControl*) is one of the PMIP entry cards in the CMIP6-
423 PMIP4 experiments (Kageyama et al., 2018; Otto-Bliesner et al., 2017) and it is therefore logical to
424 propose this period for LULC simulations. The LULC sensitivity experiment (*midHoloceneLULC*)
425 should therefore follow the CMIP6-PMIP4 protocol, that is it should be run with the same model
426 components and following the same protocols for implementing external forcings as used in the two
427 CMIP6-PMIP4 experiments (Table 1). Thus, if the *piControl* and *midHolocene* simulations is run
428 with interactive (dynamic) vegetation, then the *midHoloceneLULC* experiment should also be run
429 with dynamic vegetation in regions where there is no LULC change. For most models, this means
430 that the LULC forcing is imposed as a fraction of the grid cell and the remaining fraction of the grid
431 cell has simulated natural vegetation. These new mid-Holocene simulations would allow for a better
432 understanding of the relationship between climate changes and land-surface feedbacks (including
433 snow albedo feedbacks), and the role of water recycling at a regional scale. Thus, modelling groups
434 who are running the *midHolocene* experiment with a fully interactive carbon cycle could also run the
435 LULC experiment allowing atmospheric CO₂ to evolve interactively, subject to the simulated ocean
436 and land C balance.

437

438 The real strength of the revised LULC scenarios is to provide boundary conditions for transient
439 simulations. The CMIP6-PMIP4 simulation of 850-1850 CE (*past1000*) already incorporates LULC
440 changes as a forcing (Jungclaus et al. 2017), based on a harmonized data set that provides LULC
441 changes from 850 through to 2015 CE (Hurtt et al., 2017), which in turn draws on output from the
442 HYDE3.2 data set (Klein Goldewijk et al., 2017a). The *past1000* protocol (Jungclaus et al., 2017)
443 acknowledges that this default land-use data set is at the lower end of the spread in estimates of early
444 agricultural area indicated by other scenarios and recommends that modelling groups run additional
445 sensitivity experiments using alternative maximum and minimum scenarios. The revised scenarios
446 created by LandCover6k could be used as an alternative to these maximum and minimum scenarios.
447 Other than the substitution of the LandCover6k scenario, the specifications of other forcings would
448 then follow the recommendations for the CMIP6-PMIP4 *past1000* simulation.

449

450 A transient simulation for a longer period of the Holocene would provide a more stringent test of the
451 impact of LULC on the coupled earth system. We suggest that this transient simulation (*holotrans*)

452 should start from the pre-existing *midHolocene* simulation to capitalise on the fact that the
453 *midHolocene* simulation have been spun up for sufficiently long (Otto-Bleisner et al., 2017) to ensure
454 that the ocean and land carbon cycle is in equilibrium at the start of the transient experiment (Table
455 2). In order to be consistent with the CMIP6-PMIP4 *midHolocene* protocol (Otto-Bleisner et al.,
456 2017), changes in orbital forcing should be specified from Berger and Loutre (1991) and year-by-
457 year changes in CO₂, CH₄ and N₂O should be specified following Joos and Spahni (2008). LULC
458 changes should be implemented by imposing crop and pasture area through time as specified in the
459 revised LULC scenarios; elsewhere, the simulated vegetation should be active. It will be necessary
460 to run the Holocene transient simulation in two steps. A first simulation (*holotrans LULC*) should be
461 run using prescribed atmospheric CO₂ concentration prescribed in the atmosphere even though the
462 carbon cycle is fully interactive, because this will establish the consistency of the carbon cycle in the
463 land surface model. However, once this is done it will be possible to re-run the simulations with
464 interactive CO₂ emissions. Table 3 provides a summary of the proposed ESM simulations.
465

466 Unlike the situation for the mid-Holocene, where there is a global climate benchmark data set
467 (Bartlein et al., 2011), quantitative evaluation of the *holotrans* simulated climate can only be made
468 for key regions. Quantitative climate reconstructions through the Holocene are currently only
469 available for Europe (Davis et al., 2003) and North America (Viau et al., 2006; Viau and Gajewski,
470 2009). However, there are time series reconstructions for individual sites outside these two regions
471 (e.g. Nakagawa et al., 2002; Wilmshurst et al., 2007; Ortega-Rosas et al., 2008). Furthermore, the
472 simulated time-course of CO₂ emissions can be compared to the ice core records.
473

474 The CMIP6-PMIP4 *mid-Holocene* simulations are stylized experiments, lacking several potential
475 forcings (in addition to LULC), including changes in atmospheric dust loading, in solar irradiance,
476 and volcanic forcing. We suggest that additional sensitivity tests could be run to take these additional
477 forcings into account. In the case of solar and volcanic forcing, this would also ensure that the
478 transient *holotrans* simulations mesh seamlessly with the *past1000* simulation. Changes in solar
479 variability during the Holocene should be specified from Steinhilber et al. (2012). There are records
480 of volcanic forcing for the past 2000 years (Sigl et al., 2015; Toohey and Sigl, 2017), and these are
481 used in the *past1000* simulation. Observationally constrained estimates of the volcanic stratospheric
482 aerosol for Holocene are currently under development (M. Sigl, pers comm.) and could be
483 implemented as an additional sensitivity experiment when available. Changes in atmospheric dust
484 loading are not included in the *past1000* simulation but are important during the earlier part of the
485 Holocene (Pausata et al., 2016; Tierney et al., 2017; Messori et al., 2019). Although continuous
486 reconstructions of dust loading through the Holocene are not available, it would be possible to use
487 estimates for particular time-slices (Egerer et al., 2018) to test the sensitivity to this forcing.
488

489 **Outcomes and Perspectives**

490
491
492 LandCover6k has developed a scheme for using archaeological information to improve existing
493 scenarios of LULC changes during the Holocene, specifically by using archaeological data to provide
494 better estimates of regional population changes through time, better information on the date of
495 initiation of agriculture in a region, more regionally specific information about the type of land use,
496 and more nuanced information about land-use per capita than currently implemented in the LULC
497 scenarios generated by HYDE and KK10. While the final global data set are still in production, fast-
498 track priority products have been created and their impact on current scenarios is being tested.
499

500 Although the work of LandCover6k will provide more solid knowledge about anthropogenic
501 modification of the landscape, some information will inevitably be missing and some key regions

502 will be poorly covered. There will still be large uncertainties associated with LULC scenarios.
503 Documenting these uncertainties is an important goal of the LandCover6k project, and will allow the
504 generation of multiple scenarios comparable to the "low-end", "high-end" scenarios used for e.g. in
505 future projections. Furthermore, we have proposed a series of tests that will help to evaluate the
506 realism of the final scenarios, based on independent evidence from pollen-based reconstructions of
507 land cover, reconstructions of climate, and carbon-cycle constraints. These tests should help in
508 identifying which of the potential LULC reconstructions are most realistic and constraining the
509 sources of uncertainty.

510
511 We have proposed the use of offline vegetation-carbon-cycle simulations solely as a test of the realism
512 of the revised LULC scenario. Quantifying the LULC contribution to CO₂ emissions during the
513 Holocene would require additional simulations in which other forcings (climate, atmospheric CO₂,
514 insolation) are kept constant. The difference in simulated total terrestrial C storage between these
515 simulations and LULC simulations provides an estimate of *primary emissions* (Pongratz et al., 2014)
516 and avoids additional model uncertainty regarding the sensitivity of land C storage to atmospheric
517 CO₂ or climate being included in emission estimates. There are other sensitivity tests that would be
518 useful. For example, vegetation-carbon-cycle models differ in their ability to account for gross land
519 use transitions within grid cells (Arneeth et al., 2017). This is critical for simulating effects of non-
520 permanent agriculture where land is simultaneously abandoned and re-claimed within the extent of a
521 model grid cell. Such shifting cultivation-type agriculture implies forest degradation in areas
522 recovering from previous land use and leads to substantially higher LULC emissions compared to
523 model estimates where only net land-use changes are accounted for (Shevliakova et al., 2009). It
524 would therefore be interesting to run additional simulations accounting for net land use change, and
525 indeed separating out the effects of wood harvesting and shifting cultivation.

526
527 We anticipate that it will be possible to incorporate realistic LULC for the mid-Holocene as part of
528 the sensitivity experiments planned during PMIP4. Such experiments will complement the CMIP6-
529 PMIP4 baseline experiments, by providing insights into whether discrepancies between simulated
530 and observed 6 ka climate could be the result of incorrect specification of the land-surface boundary
531 conditions. However, the incorporation of archaeological information into LULC scenarios clearly
532 makes it possible to target other interesting periods for such experiments, for example to explore if
533 land-use changes played a role in abrupt events such as the 4.2 ka event, or to examine the impact of
534 population declines in the Americas as a consequence of European colonisation (1500-1750 CE) or
535 the changes in land use globally during the Industrial era (post 1850 CE).

536
537 In addition to providing a protocol for the PMIP 6ka sensitivity experiments, we have devised
538 a protocol for implementing the optimal LULC reconstructions for the Holocene in transient
539 experiments. The goal here is to provide one of the necessary forc- ings that could be used for
540 transient simulations in future phases of PMIP. This will allow an assessment of LULC in these
541 simulations, and therefore help address is- sues that are a focus for other MIPs e.g. LUMIP or
542 LS3MIP. When these new forcings are created, they will be made available through the PMIP4
543 website (https://pmip4.lsce.ipsl.fr/doku.php/exp_design:lgm, PMIP4 repository, 2017) and
544 the ESGF Input4MIPS repository (<https://esgf-node.llnl.gov/projects/input4mips/>, with
545 details pro- vided in the "input4MIPs summary" link). Modelling groups who run either
546 equilibrium or transient experiments following this protocol are encouraged to follow the
547 standard CMIP protocol of archiving their simulations through the ESFG.

548
549
550
551 **Acknowledgements.** LandCover 6k is a working group of the Past Global Changes (PAGES)

552 programme, which in turn received support from the Swiss Academy of Sciences. We thank PAGES
553 for their support for this activity. The land use group also received funding under the Holocene Global
554 Landuse International Focus Group of INQUA. SPH acknowledges funding from the European
555 Research Council for “GC2.0: Unlocking the past for a clearer future”. MJG thanks the Swedish
556 Strategic Research Area MERGE (Modelling the Regional and Global Earth System Model) and
557 Linnaeus University’s faculty of Health and Life Sciences (Kalmar, Sweden) for financial support.
558 We thank Joy Singarayer for providing the climate model outputs that were used to generate Figure
559 8 and Guangqi Li for assistance in producing this figure. B.D.S. was funded by ERC H2020-MSCA-
560 IF-2015, grant number 701329. The dataset for Figure 5 was generated from the ‘Cultivating
561 Societies: Assessing the Evidence for Agriculture in Neolithic Ireland’ project, supported by the
562 Heritage Council, Ireland under the INSTAR programme 2008–2010 (Reference 16682 to
563 Whitehouse, Schulting, Bogaard and McClatchie).

564
565 **Author Contributions.** SPH, MJG, BDS, MVL, KKG wrote the first draft. SPH, PB, FSRP
566 contributed to the design of the climate model experiments, BS and TK to the design of the carbon-
567 cycle simulations. The figures were contributed by JK (Fig. 1), BS (Fig. 2, Fig 9.), MVL (Fig. 3), OB
568 (Fig. 4), NJW (Fig. 5), KKG (Fig. 6), AD (Fig. 7), SPH (Fig. 8). All authors contributed to the final
569 version of the paper.

570
571 **Competing Interests.** No competing interests.

572 573 **References**

- 574 Arneth, A., Denton, F., Agus, F., Elbehri, A., Erb, K., Elasha, B.O., Rahimi, M., Rounsevell, M.,
575 Spence, A., and Valentini, R.: IPCC Special Report on Climate Change, Desertification, Land
576 Degradation, Sustainable Land Management, Food Security, and Greenhouse gas fluxes in
577 Terrestrial Ecosystems, 2019.
- 578 Arneth, A., Sitch, S., Pongratz, J., Stocker, B.D., Ciais, P., Poulter, B., Bayer, A.D., Bondeau, A.,
579 Calle, L., Chini, L.P., Gasser, T., Fader, M., Friedlingstein, P., Kato, E., Li, W., Lindeskog,
580 M., Nabel, J.E.M.S., Pugh, T.A.M., Robertson, E., Viovy, N., Yue, C., and Zaehle, S.:
581 Historical carbon dioxide emissions caused by land-use changes are possibly larger than
582 assumed, *Nature Geosci.*, 10, 79-84, doi: 10.1038/ngeo2882, 2017.
- 583 Balsera, V., Díaz-del-Río, P., Gilman, A., Uriarte, A., and Vicent, J.M.: Approaching the demography
584 of late prehistoric Iberia through summed calibrated probability distributions (7000-2000 cal
585 BC), *Quat. Int.*, 208-211, doi:10.106/j.quaint.2015.06.022, 2015.
- 586 Bartlein, P. J., Harrison, S. P., Brewer, S., Connor, S., Davis B. A. S., Gajewski, K., Guiot, J.,
587 Harrison-Prentice, T. I., Henderson, A., Peyron, O., Prentice, I. C., Scholze, M., Seppä, H.,
588 Shuman, B., Sugita, S., Thompson, R. S., Vial, A., Williams, J., and Wu, H.: Pollen-based
589 continental climate reconstructions at 6 and 21 ka: a global synthesis, *Clim. Dyn.*, 37, 775-
590 802, doi: 10.1007/s00382-010-0904-1, 2011.
- 591 Bartlein, P.J., Harrison, S.P., and Izumi, K.: Underlying causes of Eurasian mid-continental aridity
592 in simulations of mid-Holocene climate, *Geophys. Res. Lett.*, 44, doi:
593 10.1002/2017GL074476, 2017.
- 594 Barton, C.M., Ullah, I.I., and Bergin, S.: Land use, water and Mediterranean landscapes: modelling
595 long-term dynamics of complex socio-ecological systems, *Phil. Trans. R. Soc.*, A368, 5275-
596 5297, doi: 10.1098/rsta.2010.0193, 2010.
- 597 Berger, A., and Loutre, M-F.: Insolation values for the climate of the last 10 million of years, *Quat.*
598 *Sci. Rev.*, 10, 297-317, [https://doi.org/10.1016/0277-3791\(91\)90033-Q](https://doi.org/10.1016/0277-3791(91)90033-Q), 1991.
- 599 Bishop, R.R., Church, M.J., and Rowley-Conwy, P.A.: Firewood, food and human niche
600 construction: the potential role of Mesolithic hunter-gatherers in actively structuring
601 Scotland’s woodlands, *Quat. Sci. Rev.*, 108, 51-75, 2015.

- 602 Bocquet-Appel, J.-P., Naji, S., Vander Linden, M., and Kozłowski, J.K.: Detection of diffusion and
603 contact zones of early farming in Europe from the space-time distribution of ¹⁴C dates, *J.*
604 *Arch. Sci.*, 36, 807-820, doi: 10.1016/j.jas.2008.11.004, 2009.
- 605 Crema, E.R., Habu, J., Kobayashi, K., and Madella, M.: Summed probability distribution of ¹⁴C dates
606 suggests regional divergences in the population dynamics of the Jomon period in eastern Japan,
607 *PlosOne*, 11, e0154809, doi: 10.1371/journal.pone.0154809, 2016.
- 608 Davis, B.A.S., Brewer, S., Stevenson, A.C., Guiot, J., and Juggins, S.: The temperature of Europe
609 during the Holocene reconstructed from pollen data, *Quat. Sci. Rev.*, 22, 1701–1716, 2003.
- 610 Davison, K., Dolukhanov, P., Sarson, G. R., and Shukurov, P.: The role of waterways in the spread
611 of the Neolithic, *J. Arch. Sci.*, 33, 641-652, doi: 10.106/j.jas.2005.09.017, 2006.
- 612 Dawson, A., Paciorek, C.J., McLachlan, J.S., Goring, S., Williams, J.W., and Jackson, S.T.:
613 Quantifying pollen-vegetation relationships to reconstruct ancient forests using 19th-century
614 forest composition and pollen data, *Quat. Sci. Rev.*, 137, 156-175, doi:
615 [10.1016/j.quascirev.2016.01.012](https://doi.org/10.1016/j.quascirev.2016.01.012), 2016.
- 616 Dawson, A., Cao, X., Chaput, M., Hopla, E., Li, F., Edwards, M., Fyfe, R., Gajewski, K., Goring,
617 S.J., Herzschuh, U., Mazier, F., Sugita, S., Williams, J.W., Xu, Q., and Gaillard, M.-J.: Finding
618 the magnitude of human induced Northern Hemisphere land-cover transformation between 6
619 and 0.2 ka BP, *PAGES Mag.*, 26, 34-35, <https://doi.org/10.22498/pages.26.1.34>, 2018.
- 620 Egerer, S., Claussen, M., and Reick, C.: Rapid increase in simulated North Atlantic dust deposition
621 due to fast change of northwest African landscape during the Holocene, *Clim. Past*, 14, 1051-
622 1066, <https://doi.org/10.5194/cp-14-1051-2018>, 2018.
- 623 Ellis, E.C., Kaplan, J.O., Fuller, D.Q., Vavrus, S., Klein Goldewijk, K., and Verburg, P. H.: Used
624 planet: A global history, *Proc. Nat. Acad. Sci.*, 110, 7978-7985, 2013.
- 625 Elsig, J., Schmitt, J., Leuenberger, D., Schneider, R., Eyer, M., Leuenberger, M., Joos, F., Fischer,
626 H., and Stocker, T. F.: Stable isotope constraints on Holocene carbon cycle changes from an
627 Antarctic ice core, *Nature*, 461, 507-510, 2009.
- 628 Eyring, V., Bony, S., Meehl, G. A., Senior, C. A., Stevens, B., Stouffer, R. J., and Taylor, K. E.:
629 Overview of the Coupled Model Intercomparison Project Phase 6 (CMIP6) experimental design
630 and organization, *Geosci. Model Dev.*, 9, 1937–1958, [https://doi.org/10.5194/gmd-9-1937-](https://doi.org/10.5194/gmd-9-1937-2016)
631 2016, 2016.
- 632 Fischer, N., and Jungclauss, J.H.: Evolution of the seasonal temperature cycle in a transient Holocene
633 simulation: orbital forcing and sea-ice, *Clim. Past*, 7, 1139-1148, [https://doi.org/10.5194/cp-7-](https://doi.org/10.5194/cp-7-1139-2011)
634 1139-2011, 2011.
- 635 Ford, A., and Clarke, K.C.: Linking the past and present of the ancient Maya: lowland land use,
636 population distribution, and density in the Late Classic Period, in: *The Oxford Handbook of*
637 *Historical Ecology and Applied Archaeology*, Isendahl, C. and Stump, D. (eds.), doi:
638 10.1093/oxfordhb/9780199672691.013.33, 2015.
- 639 Freeman, J., Baggio, J.A., Robinson, E., Byers, D.A., Gayo, E., Finley, J.B., Meyer, J.A., Kelly, R.L.,
640 and Anderies, J.M.: Synchronisation of energy consumption by human societies throughout the
641 Holocene, *Proc. Nat. Acad. Sci.*, 115, 9962-9967, doi: 10.1073/pnas.1802859115, 2018.
- 642 Fyfe R. M., Woodbridge, J. E., and Roberts, N.: From forest to farmland: pollen-inferred land cover
643 change across Europe using the pseudobiomization approach, *Glob. Change Biol.*, 21: 1197-
644 1212, doi:10.1111/gcb.12776, 2014.
- 645 Gaillard, M.-J., Sugita, S., Mazier, F., Kaplan, J.O., Trondman, A.-K., Brostroem, A., Hickler, T.,
646 Kjellstroem, E., Kunes, P., Lemmen, C., Olofsson, J., Smith, B., and Strandberg, G.: Holocene
647 land-cover reconstructions for studies on land-cover feedbacks, *Clim. Past*, 6, 483-499,
648 <https://doi.org/10.5194/cp-6-483-2010>, 2010.
- 649 Gaillard, M.-J., Whitehouse, N., Madella, M., Morrison, K., and von Gunten, L: Past land use and
650 land cover, *PAGES Mag.*, 26, 1-44, doi:10.22498/pages.26.1, 2018.
- 651 Harrison, S.P., Bartlein, P.J., Izumi, K., Li, G., Annan, J., Hargreaves, J., Braconnot, P.B., and

- 652 Kageyama, M.: Evaluation of CMIP5 palaeo-simulations to improve climate projections,
653 *Nature Clim. Change*, 5, 735-743, 2015.
- 654 He, F., Vavrus, S.J., Kutzbach, J.E., Ruddiman, W.F., Kaplan, J.O., and Krumhardt, K.M.: Simulating
655 global and local surface temperature changes due to Holocene anthropogenic land cover
656 change, *Geophys. Res. Lett.*, 41, 623–631, 2014.
- 657 Hellman, S., Gaillard, M.-J., Broström, A., and Sugita, S.: The REVEALS model, new tool to
658 estimate past regional plant abundance from pollen data in large lakes: validation in southern
659 Sweden, *J. Quat. Sci.*, 22, 1-22, 2008a.
- 660 Hellman, S., Gaillard M.-J., Broström, A., and Sugita, S.: Effects of the sampling design and selection
661 of parameter values on pollen-based quantitative reconstructions of regional vegetation: a case
662 study in southern Sweden using the REVEALS model, *Veg. History Archaeobot.*, 17, 445-460,
663 2008b.
- 664 Herrero, M., Havlík, P., Valin, H., Notenbaert, A., Rufino, M.C., Thornton, P.K., Blümmel, M.,
665 Weiss, F., Grace, D., and Obersteiner, M.: Biomass use, production, feed efficiencies, and
666 greenhouse gas emissions from global livestock systems, *Proc. Nat. Acad. Sci.*, 110, 20888-
667 20893, 2013.
- 668 Hughes, R.E., Weiberg, E., Bonnier, A., Finne, M., and Kaplan, J.O.: Quantifying land use in past
669 societies from cultural practice and archaeological data, *Land*, 7, 9,
670 doi.org/10.3390/land/7010009, 2018.
- 671 Hurtt, G., Chini, L., Sahajpal, R., Frolking, S., Calvin, K., Fujimori, S., Klein Goldewijk, K.,
672 Hasegawa, T., Havlik, P., Lawrence, D., Lawrence, P., Popp, A., Stehfest, E., van Vuuren, D.,
673 and Zhang, X.: Harmonization of global land-use change and management for the period 850–
674 2100, *Geosci. Model Dev. Discuss.*, 2017.
- 675 Janssen, E., Poblome, J., Claeys, J., Kint, V., Degryse, P., Marinova, E., and Muys, B.: Fuel for
676 debating ancient economies. Calculating wood consumption at urban scale in Roman Imperial
677 times, *J. Arch. Sci.: Reports*, 11, 592-599, 2017.
- 678 Joos, F., and Spahni, R.: Rates of change in natural and anthropogenic radiative forcing over the past
679 20,000 years, *Proc. Nat. Acad. Sci.*, 105, 1425–1430, 2008.
- 680 Joos, F., Gerber, S., Prentice, I.C., Otto-Bliesner, B.L., and Valdes, P.J.: Transient simulations of
681 Holocene atmospheric carbon dioxide and terrestrial carbon since the last glacial maximum,
682 *Global Biogeochem. Cy.*, 18, GB2002, doi:10.1029/2003GB002156, 2004.
- 683 Jungclaus, J.H., Bard, E., Baroni, M., Braconnot, P., Cao, J., Chini, L. P., Egorova, T., Evans, M.,
684 González-Rouco, J.F., Goosse, H., Hurtt, G.C., Joos, F., Kaplan, J. O., Khodri, M., Klein
685 Goldewijk, K., Krivova, N., LeGrande, A.N., Lorenz, S. J., Luterbacher, J., Man, W., Maycock,
686 A.C., Meinshausen, M., Moberg, A., Muscheler, R., Nehrbass-Ahles, C., Otto-Bliesner, B.I.,
687 Phipps, S.J., Pongratz, J., Rozanov, E., Schmidt, G.A., Schmidt, H., Schmutz, W., Schurer, A.,
688 Shapiro, A.I., Sigl, M., Smerdon, J.E., Solanki, S.K., Timmreck, C., Toohey, M., Usoskin, I.G.,
689 Wagner, S., Wu, C.-J., Yeo, K.L., Zanchettin, D., Zhang, Q., and Zorita, E.: The PMIP4
690 contribution to CMIP6 – Part 3: The last millennium, scientific objective, and experimental
691 design for the PMIP4 past1000 simulations, *Geosci. Model Dev.*, 10, 4005–4033,
692 <https://doi.org/10.5194/gmd-10-4005-2017>, 2017.
- 693 Kageyama, M., Braconnot, P., Harrison, S.P., Haywood, A., Jungclaus, J., Otto-Bliesner, B.,
694 Peterschmitt, J.-Y., Abe-Ouchi, A., Albani, S., Bartlein, P., Brierley, C., Crucifix, M., Dolan,
695 A., Fernandez-Donado, L., Fischer, H., Hopcroft, P., Ivanovic, R., Lambert, F., Lunt, D.,
696 Mahowald, N., Peltier, W.R., Phipps, S., Roche, D., Schmidt, G., Tarasov, L., Valdes, P.,
697 Zhang, Q., and Zhou, T.: The PMIP4 contribution to CMIP6 – Part 1: Overview and over-
698 arching analysis plan. *Geosci. Model Dev.*, 11: 1033-1057. [https://doi.org/10.5194/gmd-11-
699 1033-2018](https://doi.org/10.5194/gmd-11-1033-2018), 2018.
- 700 Kaplan, J.O., Krumhardt, K.M., Ellis, E.C., Ruddiman, W.F., Lemmen, C., and Klein Goldewijk, K.:
701 Holocene carbon emissions as a result of anthropogenic land cover change, *Holocene*, 21, 775-

702 791, 2011.

703 Kaplan, J.O., Krumhardt, K.M., Gaillard, M.-J., Sugita, S., Trondman, A.-K., Fyfe, R., Marquer, L.,
704 Mazier, F., and Nielsen, A.B.: Constraining the deforestation history of Europe: Evaluation of
705 historical land use scenarios with pollen-based land cover reconstructions, *Land*, 6, 9,
706 doi:10.3390/land6040091, 2017.

707 Kay, A. U., Fuller, D. Q., Neumann, K., Eichhorn, B., Höhn, A., Morin-Rivat, J., Champion, L.,
708 Linseele, V., Huysecom, E., Ozainne, S., Lespez, L., Biagetti, S., Madella, M., Salzmann, U.,
709 and Kaplan, J. O.: Diversification, intensification, and specialization: Changing land use in
710 western Africa from 1800 BC to AD 1500, *J. World Prehistory*, in press.

711 Klein Goldewijk, K., Beusen, A., van Drecht, G., and de Vos, M.: The HYDE 3.1 spatially explicit
712 database of human induced land use change over the past 12,000 years, *Glob. Ecol. Biogeog.*,
713 20, 73-86, 2011.

714 Klein Goldewijk, K., Beusen, A., Doelman, J., and Stehfest, E.: Anthropogenic land-use estimates
715 for the Holocene; HYDE 3.2, *Earth Syst. Sci. Data*, 9, 927-953, <https://doi.org/10.5194/essd-9-1-2017>, 2017a.

716 Klein Goldewijk, K., Dekker, S.C., and van Zanden, J.L.: Per-capita estimations of long-term
717 historical land use and the consequences for global change research, *J. Land Use Sci.*, 12,
718 313-337, <https://doi.org/10.1080/1747423X.2017.1354938>, 2017b.

720 Lawrence, D.M., Hurtt, G.C., Arneth, A., Brovkin, V., Calvin, K.V., Jones, A.D., Jones, C.D.,
721 Lawrence, P.J., de Noblet-Ducoudré, N., Pongratz, J., Seneviratne, S.I., and Shevliakova, E.:
722 The Land Use Model Intercomparison Project (LUMIP) contribution to CMIP6: rationale and
723 experimental design, *Geosci. Model Dev.*, 9, 2973-2998, [https://doi.org/10.5194/gmd-9-2973-](https://doi.org/10.5194/gmd-9-2973-2016)
724 2016, 2016.

725 Le Quéré, C., Andrew, R.M., Friedlingstein, P., Sitch, S., Hauck, J., Pongratz, J., Pickers, P.A.,
726 Korsbakken, J.I., Peters, G.P., Canadell, J.G., Arneth, A., Arora, V.K., Barbero, L., Bastos, A.,
727 Bopp, L., Chevallier, F., Chini, L.P., Ciais, P., Doney, S.C., Gkritzalis, T., Goll, D.S., Harris,
728 I., Haverd, V., Hoffman, F.M., Hoppema, M., Houghton, R.A., Hurtt, G., Ilyina, T., Jain, A.K.,
729 Johannessen, T., Jones, C.D., Kato, E., Keeling, R.F., Goldewijk, K.K., Landschützer, P.,
730 Lefèvre, N., Lienert, S., Liu, Z., Lombardozzi, D., Metzl, N., Munro, D.R., Nabel, J.E.M.S.,
731 Nakaoka, S.-I., Neill, C., Olsen, A., Ono, T., Patra, P., Pregon, A., Peters, W., Peylin, P., Pfeil,
732 B., Pierrot, D., Poulter, B., Rehder, G., Resplandy, L., Robertson, E., Rocher, M., Rödenbeck,
733 C., Schuster, U., Schwinger, J., Séférian, R., Skjelvan, I., Steinhoff, T., Sutton, A., Tans, P.P.,
734 Tian, H., Tilbrook, B., Tubiello, F. N., van der Laan-Luijkx, I.T., van der Werf, G.R., Viovy,
735 N., Walker, A.P., Wiltshire, A.J., Wright, R., Zaehle, S., and Zheng, B.: Global Carbon Budget
736 2018, *Earth Syst. Sci. Data*, 10, 2141-2194, <https://doi.org/10.5194/essd-10-2141-2018>, 2018.

737 Loisel, J., Yu, Z., Beilman, D.W., Camill, P., Alm, J., Amesbury, M.J., Anderson, D., Andersson, S.,
738 Bochicchio, C., Barber, K., Belyea, L.R., Bunbury, J., Chambers, F.M., Charman, D.J.,
739 Vleeschouwer, F.D., Fiałkiewicz-Kozielec, B., Finkelstein, S.A., Gałka, M., Garneau, M.,
740 Hammarlund, D., Hinchcliffe, W., Holmquist, J., Hughes, P., Jones, M.C., Klein, E.S., Kokfelt,
741 U., Korhola, A., Kuhry, P., Lamarre, A., Lamentowicz, M., Large, D., Lavoie, M., MacDonald,
742 G., Magnan, G., Mäkilä, M., Mallon, G., Mathijssen, P., Mauquoy, D., McCarroll, J., Moore,
743 T.R., Nichols, J., O'Reilly, B., Oksanen, P., Packalen, M., Peteet, D., Richard, P.J., Robinson,
744 S., Ronkainen, T., Rundgren, M., Sannel, A.B.K., Tarnocai, C., Thom, T., Tuittila, E.-S.,
745 Turetsky, M., Väliranta, M., and der Linden, M., van Geel B., van Bellen, S., Vitt, D., Zhao,
746 Y., and Zhou, W.: A database and synthesis of northern peatland soil properties and Holocene
747 carbon and nitrogen accumulation, *Holocene*, 24, 1028-1042, 2014.

748 Lyman, R. L.: *Quantitative Paleozoology*. Cambridge University Press, 2008.

749 Maezumi, S.Y., Robinson, M., de Souza, J., Urrego, D.H., Schaan, D., Alves, D., and Iriarte, J.: New
750 insights from pre-Columbian land use and fire management in Amazonian Dark Earth forests,
751 *Front. Ecol. Evol.*, 6, 111, doi: 10.3389/fevo.2018.00111, 2018.

- 752 Mahowald, N.M., Randerson, J.T., Lindsay, K., Munoz, E., Doney, S.C., Lawrence, P.,
753 Schlunegger, S., Ward, D.S., Lawrence, D., and Hoffman, F. M.: Interactions between land use
754 change and carbon cycle feedbacks, *Glob. Biogeochem. Cy.*, 31, 96–113,
755 doi:10.1002/2016GB005374, 2017.
- 756 Marston, J.M.: Modeling wood acquisition strategies from archaeological charcoal remains, *J. Arch.*
757 *Sci.*, 36, 2192-2200, 2009.
- 758 Marston, J.M., Holdaway, S.J., and Wendrich, W.: Early- and middle-Holocene wood exploitation in
759 the Fayum basin, Egypt, *Holocene*, 27, 1812-1824, 2017.
- 760 Mauri, A., Davis, B. A. S., Collins, P. M., and Kaplan, J. O.: The influence of atmospheric circulation
761 on the mid-Holocene climate of Europe: a data–model comparison, *Clim. Past*, 10, 1925–1938,
762 <https://doi.org/10.5194/cp-10-1925-2014>, 2014.
- 763 Mazoyer, M., and Roudart, L.: *A History of World Agriculture: From the Neolithic to the Current*
764 *Crisis*. Earthscan, UK, 2006.
- 765 McGrath, M. J., Luyssaert, S., Meyfroidt, P., Kaplan, J. O., Burgi, M., Chen, Y., Erb, K., Gimmi, U.,
766 McInerney, D., Naudts, K., Otto, J., Pasztor, F., Ryder, J., Schelhaas, M. J., and Valade, A.:
767 Reconstructing European forest management from 1600 to 2010, *Biogeosci.*, 12, 4291-4316.
768 doi:10.5194/bg-12-4291-2015, 2015.
- 769 McLaughlin, T. R., Whitehouse, N. J., Schulting, R. J., McClatchie, M., Barratt, P. and Bogaard, A.:
770 The changing face of Neolithic and Bronze Age Ireland: A big data approach to the
771 settlement and burial records. *J. World Prehist.*, 29, 117-153. doi:10.1007/s10963-016-
772 9093-0, 2016.
- 773 Messori, G., Gaetani, M., Zhang, Q., Zhang, Q., and Pausata, F. S. R.: The water cycle of the mid-
774 Holocene West African monsoon: The role of vegetation and dust emission changes, *Int. J.*
775 *Climatol.*, 39, 1927– 1939, <https://doi.org/10.1002/joc.5924>, 2019.
- 776 Mitchell, L., Brook, E., Lee, J., Buizert, C., and Sowers, T.: Constraints on the late Holocene
777 anthropogenic contribution to the atmospheric methane budget, *Science*, 342, 964–966,
778 doi:10.1126/science.1238920, 2013.
- 779 Morrison, K.D., Hammer, E., Popova, L., Madella, M., Whitehouse, N., Gaillard, M.-J. and
780 LandCover6k Land-Use Group Members: Global-scale comparisons of human land use:
781 developing shared terminology for land-use practices for global changes, *PAGES Mag.*, 26, 8-
782 9, 2018.
- 783 Myhre, G., Shindell, D., Bréon, F.-M., Collins, W., Fuglestedt, J., Huang, J., Koch, D., Lamarque,
784 J.-F., Lee, D., Mendoza, B., Nakajima, T., Robock, A., Stephens, G., Takemura T., and Zhang,
785 H.: Anthropogenic and natural radiative forcing. in: *Climate Change 2013: The Physical*
786 *Science Basis*. Contribution of Working Group I to the Fifth Assessment Report of the
787 Intergovernmental Panel on Climate Change (T F Stocker, D Qin, G-K Plattner, M Tignor, S
788 K Allen, J Boschung, A Nauels, Y Xia, V Bex and P M Midgley (eds), Cambridge: Cambridge
789 University Press Cambridge, United Kingdom and New York, NY, USA, 2013.
- 790 Nakagawa, T., Tarasov, P.E., Nishida, K., Gotanda, K., and Yasuda, Y.: Quantitative pollen-based
791 climate reconstruction in central Japan: application to surface and Late Quaternary spectra,
792 *Quat. Sci. Rev.*, 21, 2099–2113, 2002.
- 793 Nielsen, A.B., Giesecke, T., Theuerkauf, M., Feeser, I., Behre, K.-H., Beug, H.-J., Chen, S.-H.,
794 Christiansen, J., Dörfler, W., Endtmann, E., Jahns, S., de Klerk, O., Köhl, N., Latałowa, M.,
795 Odgaard, B.V., Rasmussen, P., Stockholm, J.R., Voigt, R., Wiethold, J., and Wolters, S.:
796 Quantitative reconstructions of changes in regional openness in north-central Europe reveal
797 new insights into old questions, *Quat. Sci. Rev.*, 47, 131–149, 2012.
- 798 Oh, Y., Conte, M., Kang, S., Kim, J., and Hwang, J.: Population fluctuation and the adoption of food
799 production in prehistoric Korea: using radiocarbon dates as a proxy for population change,
800 *Radiocarbon*, 59, 1761-1770, doi: 10.1017/RDC.2017.1.22, 2017.
- 801 Ortega-Rosas, C.I., Guiot, J., Penalba, M.C., Ortiz-Acosta, M.E.: Biomization and quantitative

802 climate reconstruction techniques in northwestern Mexico—with an application to four
803 Holocene pollen sequences, *Glob. Planet. Change*, 61, 242–266, 2008.

804 Orton, D., Gaastra, J., and Vander Linden, M.: Between the Danube and the Deep Blue Sea:
805 zooarchaeological meta-analysis reveals variability in the spread and development of Neolithic
806 farming across the western Balkans, *Open Quat.*, 2, doi: 10.5334/oq.28, 2016.

807 Otto-Bliesner, B.L., Braconnot, P., Harrison, S.P., Lunt, D.J., Abe-Ouchi, A., Albani, S., Bartlein,
808 P.J., Capron, E., Carlson, A.E., Dutton, A., Fischer, H., Goelzer, H., Govin, A., Haywood, A.,
809 Joos, F., Legrande, A.N., Lipscomb, W.H., Lohmann, G., Mahowald, N., Nehrbass-Ahles, C.,
810 Pausata, F.S.R., Peterschmidt, J.-Y., Phipps, S.J., Renssen, R., and Zhang, Q.: The PMIP4
811 contribution to CMIP6 – Part 2: Two interglacials, scientific objective and experimental design
812 for Holocene and Last Interglacial simulations. *Geosci. Mod. Dev.*, 10, 3979-4003,
813 <https://doi.org/10.5194/gmd-10-1-2017>, 2017.

814 Pausata, F.S.R., Messori, G., Zhang, Q.: Impacts of dust reduction on the northward expansion of the
815 African monsoon during the Green Sahara period, *Earth Planet. Sci. Lett.*, 434, 298-
816 307, <https://doi.org/10.1016/j.epsl.2015.11.049>, 2016.

817 Perugini, L. Caporaso, L., Marconi, S., Cescatti, A., Quesada, B., de Noblet-Ducoudré, N., House,
818 J.I., and Arneth, A.: Biophysical effects on temperature and precipitation due to land cover
819 change, *Environ. Research Lett.*, 12, 053002, <https://doi.org/10.1088/1748-9326/aa6b3f>, 2017.

820 Phelps, L.N., and Kaplan, J.O.: Land use for animal production in global change studies: Defining
821 and characterizing a framework, *Glob Chang Biol*, 23, 4457-4471, 10.1111/gcb.13732, 2017.

822 Pirzamanbein, B., Lindström, J., Poska, A., Sugita, S., Trondman, A., Fyfe, R., Mazier, F., Nielsen,
823 A.B., Kaplan, J.O., Bjune, A.E., Birks, H.J.B., Giesecke, T., Kangur, M., Latałowa, M.,
824 Marquer, L., Smith, B., and Gaillard, M.-J.: Creating spatially continuous maps of past land
825 cover from point estimates: A new statistical approach applied to pollen data, *Ecol. Complexity*,
826 20, 127-141, 2014.

827 Pirzamanbein, B., Lindström, J., Poska, A., and Gaillard, M.-J.: Modelling spatial compositional data:
828 Reconstructions of past land cover and uncertainties, *Spatial Stat.*, 24, 14–31, 2018.

829 Pongratz, J., Reick, C., Raddatz, T., and Claussen, M.: A reconstruction of global agricultural areas
830 and land cover for the last millennium, *Glob. Biogeochem. Cy.*, 22, 2008.

831 Pongratz, J., Reick, C.H., Raddatz, T., and Claussen, M.: Biogeophysical versus biogeochemical
832 climate response to historical anthropogenic land cover change, *Geophys. Res. Lett.*, 37,
833 L08702, doi:10.1029/2010GL043010, 2010.

834 Pongratz, J., Reick, C. H., Houghton, R. A., and J. I. House, J. I.: Terminology as a key uncertainty
835 in net land use and land cover change carbon flux estimates, *Earth Syst. Dynam.*, 5, 177–195,
836 www.earth-syst-dynam.net/5/177/2014/ doi:10.5194/esd-5-177-2014, 2014.

837 Ramankutty, N., and Foley, J.A.: Estimating historical changes in global land cover: Croplands from
838 1700 to 1992, *Glob. Biogeochem. Cy.*, 13, 997-1027, 1999.

839 Reitz, E. J., and Wing E.S.: *Zooarchaeology*. Cambridge University Press, 2008.

840 Rick, J.W.: Dates as data: an examination of the Peruvian Pre-ceramic radiocarbon record, *Am. Antiq.*,
841 52, 55–73, 1987.

842 Robinson, E., Zahid, H.J., Coddling, B.F., Haas, R., and Kelly, R.L.: Spatiotemporal dynamics of
843 prehistoric human population growth: radiocarbon ‘dates as data’ and population ecology
844 models, *J. Arch. Sci.*, 101, 63-71, 2019.

845 Ruddiman, W. F.: The anthropogenic greenhouse era began thousands of years ago, *Clim. Change*,
846 61, 261–293, doi:10.1023/B:CLIM.0000004577.17928.fa, 2003.

847 Russell, T., Silva, F., and Steele, J.: Modelling the spread of farming in the Bantu-speaking regions
848 of Africa: an archaeology-based phylogeography, *PlosONE*, 9, e87584, doi:
849 10.1371/journal.pone.0087584, 2014.

850 Shennan, S., Downey, S.S., Timpson, A., Edinborough, K., Colledge, S., Kerig, T., Manning, K., and
851 Thomas, M.G.: Regional population collapse followed initial agriculture booms in mid-

852 Holocene Europe, *Nat. Comms.*, 4, 248., doi: 10.1038/ncomms3486, 2013.

853 Shevliakova, E., Pacala, S. W., Malyshev, S., Hurtt, G. C., Milly, P. C. D., Caspersen, J. P., Sentman,
854 L. T., Fisk, J. P., Wirth, C., and Crevoisier, C.: Carbon cycling under 300 years of land use
855 change: Importance of the secondary vegetation sink, *Glob. Biogeochem. Cy.*, 23, GB2022,
856 doi:10.1029/2007GB003176, 2009.

857 Sigl, M., Winstrup, M., McConnell, J.R., Welten, K.C., Plunkett, G., Ludlow, F., Büntgen, U., Caffee,
858 M., Chellman, N., Dahl-Jensen, D., Fischer, H., Kipfstuhl, S., Kostick, C., Maselli, O.J.,
859 Mekhaldi, F., Mulvaney, R., Muscheler, R., Pasteris, D.R., Pilcher, J.R., Salzer, M., Schüpbach,
860 S., Steffensen, J.P., Vinther, B.M., and Woodruff, T.E.: Timing and climate forcing of volcanic
861 eruptions for the past 2,500 years, *Nature*, 523, 543–549, <https://doi.org/10.1038/nature14565>,
862 2015.

863 Silva, F., and Steele, J.: New methods for reconstructing geographical effects on dispersal rates from
864 large-scale radiocarbon databases, *J. Arch. Sci.*, 52, 609-620, doi: 10.1016/j.jas.2014.04.021,
865 2014.

866 Silva, F., and Vander Linden, M.: Amplitude of travelling front as inferred from ¹⁴C predicts levels
867 of genetic admixture among European early farmers, *Sci. Reports*, 7, 11985, doi:
868 10.1038/s41598-017-12318-2, 2017.

869 Silva, F., Stevens, C.J., Weisskopf, A., Castillo, C., Qin, L., Bevan, A., and Fuller, D.Q.: Modelling
870 the geographical origin of rice cultivation in Asia using the Rice Archaeological Database,
871 *PlosOne*, 10, e0137024, 2015.

872 Singarayer, J.S., Valdes, P.J., Friedlingstein, P., Nelson, S., and Beerling, D.J.: Late Holocene
873 methane rise caused by orbitally controlled increase in tropical sources, *Nature*, 470, 82– 85,
874 doi:10.1038/nature09739, 2011.

875 Smith, M.C., Singarayer, J.S., Valdes, P.J., Kaplan, J.O., and Branch, N.P.: The biogeophysical
876 climatic impacts of anthropogenic land use change during the Holocene, *Clim. Past*, 12, 923-
877 941, doi: <https://doi.org/10.5194/cp-12-923-2016>, 2016.

878 Steinhilber, F., Abreu, J. A., Beer, J., Brunner, I., Christl, M., Fischer, H., Heikkilä, U., Kubik, P. W.,
879 Mann, M., McCracken, K.G., Miller, H., Miyahara, H., Oerter, H., and Wilhelms, F.: 9400
880 years of cosmic radiation and solar activity from ice cores and tree rings, *Proc. Natl. Acad. Sci.*,
881 109, 5967–5971, 2012.

882 Stocker, B. D., Strassmann, K., and Joos, F.: Sensitivity of Holocene atmospheric CO₂ and the
883 modern carbon budget to early human land use: analyses with a process-based model,
884 *Biogeosci.*, 8, 69-88, doi:10.5194/bg-8-69-2011, 2011.

885 Stocker, B.D., Yu, Z., Massa, C., and Joos, F.: Holocene peatland and ice-core data constraints on
886 the timing and magnitude of CO₂ emissions from past land use, *Proc. Natl. Acad. Sci.*, 114,
887 1492-1497, doi:10.1073/pnas.1613889114, 2017.

888 Styring, A., Rösch, M., Stephan, E., Stika, H.-P., Fischer, E., Sillmann, E., and Bogaard, A.:
889 Centralisation and long-term change in farming regimes: comparing agricultural practices in
890 Neolithic and Iron Age south-west Germany, *Proc. Prehist. Soc.*, 83: 357-381, doi:
891 10.1017/ppr.2017.3, 2017.

892 Sugita, S.: Theory of quantitative reconstruction of vegetation I: pollen from large sites REVEALS
893 regional vegetation composition, *Holocene*, 17, 229–241, 2007.

894 Tarasov, P., Williams, J.W., Andreev, A., Nakagawa, T., Bezrukova, E., Herzschuh, U., Igarashi, Y.,
895 Müller, S., Werner, K., and Zheng, Z.: Satellite- and pollen-based quantitative woody cover
896 reconstructions for northern Asia: Verification and application to late-Quaternary pollen data,
897 *Earth Planet. Sci. Lett.*, 264, 284–298, 2007.

898 Tauger, M.B: *Agriculture in World History*, Routledge, 2013.

899 Tierney, J.E., Pausata, F.S.R., and deMenocal, P.B.: Rainfall regimes of the Green Sahara, *Sci.*
900 *Advan.*, 3, e1601503, 2017.

901 Timpson, A., Colledge, S., Crema, E., Edinborough, K., Kerig, T., Manning, K., Thomas, M. G. &

- 902 Shennan, S.: Reconstructing regional population fluctuations in the European Neolithic using
 903 radiocarbon dates: a new case-study using an improved method, *J. Arch. Sci.*, 52, 549-557, doi:
 904 10.1016/j.jas.2014.08.011, 2014.
- 905 Toohey, M. and Sigl, M.: Volcanic stratospheric sulphur injections and aerosol optical depth from
 906 500 BCE to 1900 CE, *Earth Syst. Sci. Data*, 9, 809-831, [https://doi.org/10.5194/essd-9-809-](https://doi.org/10.5194/essd-9-809-2017)
 907 [2017](https://doi.org/10.5194/essd-9-809-2017), 2017.
- 908 Trondman, A. K., Gaillard, M.-J., Mazier, F., Sugita, S., Fyfe, R., Nielsen, A.B., Twiddle, C., Barratt,
 909 P., Birks, H.J.B., Bjune, A. E., Björkman, L., Broström, A., Caseldine, C., David, R., Dodson,
 910 J., Dörfler, W., Fischer, E., van Geel, B., Giesecke, T., Hultberg, T., Kalnina, L., Kangur, M.,
 911 van der Knaap, P., Koff, T., Kuneš, P., Lagerås, P., Latałowa, M., Lechterbeck, J., Leroyer, C.,
 912 Leydet, M., Lindbladh, M., Marquer, L., Mitchell, F.J. G., Odgaard, B.V., Peglar, S.M.,
 913 Persson, T., Poska, A., Rösch, M., Seppä, H., Veski, S., and Wick, L.: Pollen-based quantitative
 914 reconstructions of Holocene regional vegetation cover (plant-functional types and land-cover
 915 types) in Europe suitable for climate modelling, *Glob. Change Biol.*, 21, 676-697,
 916 doi:10.1111/gcb.12737, 2015.
- 917 Trondman, A.-K., Gaillard, M.-J., Sugita, S., Björkman, L., Greisman, A., Hultberg, T., Lagerås, P.,
 918 and Lindbladh, M.: Are pollen records from small sites appropriate for REVEALS model-based
 919 quantitative reconstructions of past regional vegetation? An empirical test in southern Sweden,
 920 *Veget. Hist. Archaeobot.*, 25, 131–151, doi: 10.1007/s00334-015-0536-9, 2016.
- 921 van den Hurk, B., Kim, H., Krinner, G., Seneviratne, S.I., Derksen, C., Oki, T., Douville, H., Colin,
 922 J., Ducharne, A., Cheruy, F., Viovy, N., Puma, M.J., Wada, Y., Li, W., Jia, B., Alessandri, A.,
 923 Lawrence, D.M., Weedon, G.P., Ellis, R., Hagemann, S., Mao, J., Flanner, M.G., Zampieri, M.,
 924 Materia, S., Law, R.M., and Sheffield, J.: LS3MIP (v1.0) contribution to CMIP6: the Land
 925 Surface, Snow and Soil moisture Model Intercomparison Project – aims, setup and expected
 926 outcome, *Geosci. Model Dev.*, 9, 2809-2832, <https://doi.org/10.5194/gmd-9-2809-2016>, 2016.
- 927 Vavrus, S., Ruddiman, W.F., and Kutzbach, J.E.: Climate model tests of the anthropogenic influence
 928 on greenhouse-induced climate change: the role of early human agriculture, industrialization,
 929 and vegetation feedbacks, *Quat. Sci. Rev.*, 27, 1410-1425, 2008.
- 930 Veal, R., 2017. Wood and charcoal for Rome: towards an understanding of ancient regional fuel
 931 economics, In de Haas, T. & Gijs, T. (eds), *Rural communities in a globalizing economy: new*
 932 *perspectives on the economic integration of Roman Italy*, Brill, (New York and Leiden):
 933 pp.388-406.
- 934 Viau, A.E., and Gajewski, K.: Reconstructing millennial, regional paleoclimates of boreal Canada
 935 during the Holocene, *J. Clim.*, 22, 316–330, 2009.
- 936 Viau, A., Gajewski, K., Sawada, M., and Fines, P.: Mean-continental July temperature variability in
 937 North America during the past 14,000 years, *J. Geophys. Res. Atmos.*, 111, D09102,
 938 doi:10.1029/2005JD006031, 2006
- 939 Weiberg, E., Hughes, R. E., Finné, M., Bonnier, A., and Kaplan, J. O.: Mediterranean land use
 940 systems from prehistory to antiquity: a case study from Peloponnese (Greece), *J. Land Use Sci.*,
 941 1-20, doi:10.1080/1747423x.2019.1639836, 2019.
- 942 Whitehouse, N., Schulting, R. J., McClatchie, M., Barratt, P., LcLaughlin, T.R., Bogaard, A.,
 943 Colledge, S., Marchant, R., Gaffrey, J., and Bunting, M.J.: Neolithic agriculture on the
 944 European western frontier: the boom and bust of early farming in Ireland, *J. Arch. Sci.*, 51, 181-
 945 205, doi: 10.1016/j.jas.2013.08.009, 2014.
- 946 Williams, A.: The use of summed radiocarbon probability distributions in archaeology: a review of
 947 methods. *J. Archaeol. Sci.*, 39, 578–589, <https://doi.org/10.1016/j.jas.2011.07.014>, 2012.
- 948 Wilmshurst, J.M., McGlone, M.S., Leathwick, J.R., and Newnham, R.M.: A pre-deforestation pollen-
 949 climate calibration model for New Zealand and quantitative temperature reconstructions for the
 950 past 18000 years BP, *J. Quat. Sci.*, 22, 535–547, 2007.
- 951 Wright, P.: Preservation or destruction of plant remains by carbonization. *J.Arch.Sci* 30, 577-583,

952 doi: 10.1016/S0305-4403(02)00203-0, 2003.
953 Zahid, H.J., Robinson, E., and Kelly, R.L.: Agriculture, population growth, and statistical analysis of
954 the radiocarbon record, *Proc. Natl. Acad. Sci.*, 113, 931-935, doi: 10.1073/pnas.1517650112,
955 2016.
956 Zanon, M., Davis, B.A.S., Marquer, L., Brewer, S., and Kaplan, J.O.: European forest cover during
957 the past 12,000 years: a palynological reconstruction based on modern analogs and remote
958 sensing, *Front. Plant Sci.*, 9, 253, doi: 10.3389/fpls.201800253, 2018.
959 Zimmermann, A., Wendt, K.P., and Hilpert, J.: Landscape archaeology in central Europe. *Proc.*
960 *Prehist. Soc.*, 75, 1-53, doi: 10.1017/S007949X00000281, 2009.
961 Zohary, D., Hopf, M., and Weiss, E.: *Domestication of Plants in the Old World: The Origin and*
962 *Spread of Domesticated Plants in South-west Asia, Europe, and the Mediterranean Basin*, 4th
963 *Edn.*, Oxford University Press, Oxford, 2012.
964
965

966 **Figure and Table Captions**

967

968 Figure 1: Land use at ca 6000 years ago (6ka BP, 4000 years BCE) from the two widely used global
969 historical land-use scenarios HYDE 3.2 (top panel, Klein Goldewijk et al. 2017a) and KK10 (bottom
970 panel, Kaplan et al. 2011), illustrating the large disagreement between LULC scenarios at a regional
971 scale. In both scenarios, the land-sea mask and lake areas are for the present day.

972

973 Figure 2: Proposed scheme for developing robust LULC scenarios through iterative testing and
974 refinement, as input to Earth System Model (ESM) simulations. The archaeological inputs developed
975 in Phase 1 can be used independently or together to improve the LULC reconstructions; iterative
976 testing of the LULC scenario reconstruction (Phase 2) will ensure that these inputs are reliable before
977 they are used of ESM simulations (Phase 3). The uppermost three LULC simulations capitalize on
978 already planned baseline simulations without LULC; the lowermost two simulations are envisaged
979 as new sensitivity experiments.

980

981 Figure 3: Reconstruction of changes in population size in the Iberian Peninsula during the Holocene
982 (9000 to 2000 BP, 9ka to 2ka BP) using summed probability distributions (SPDs) of radiocarbon
983 dates (data after Balsera et al., 2015). The red line indicates the onset of agriculture in the region. The
984 lower panels show areas under human use at 6ka (left) and 4ka (right) using kernel density estimates,
985 where the white dots are actual archaeological sites and the shading shows the implied density of
986 occupation.

987

988 Figure 4: The hierarchical scheme of land-use classes used for global mapping in LandCover6k
989 (updated from Morrison et al, 2018).

990

991 Figure 5: An example of regional land-use mapping. The upper panels show the distribution of known
992 archaeological sites superimposed on kernel density estimates of the extent of land-use based on the
993 density of observations, and the lower panels show these data superimposed on the LandCover6k
994 land-use classes for the Middle Neolithic (3600-3400 years BCE, 5600-5400 years BP, 5.6-5.4 ka
995 BP) (left panels) and the Early Neolithic (3750-3600 years BCE, 5750-5600 years BP, 5.7-5.6 ka BP)
996 (right panels) of Ireland. Data points derive from ¹⁴C dated archaeological sites and distributions of
997 settlements and monuments that have been assigned to each archaeological period following the
998 dataset published in McLaughlin et al. (2016). The assigned land-use classes are inferred from
999 archaeological material from one (or more) sites within the grid box. It should not be assumed that
1000 the whole gridcell was being used for agriculture during the Middle and Early Neolithic. Informed
1001 assessment suggests that agricultural land (crop growing and grazing, combined) probably occupied
1002 between 10-15% of the total grid area in the low-level food production regions of the eastern and
1003 western coastal areas, whilst agricultural land likely represents 5% or less of the total grid cell area
1004 in inland areas.

1005

1006 Figure 6: Schematic illustration of the proposed implementation of ¹⁴C-based population estimates,
1007 date of first agriculture, land-use maps, and land-use per capita information in the HYDE model (here
1008 indicated as HYDE3.x). The archaeological data are represented as values for a grid cell in geographic
1009 space at a given time for date of first agriculture and land use, but as a time series for a specific grid
1010 cell for population and land-use per capita. In the case of population estimates, date of first agriculture
1011 and land-use per capita data, we show the initial estimate and the revised estimate after taking the
1012 archaeological information into account in the HYDE3.x plot. It should be assumed in the case of the
1013 land-use mapping that the original estimate was that there was no land use in this region.

1014

1015 Figure 7: Northern extratropical (>40°N) mean fractional cover of open land at 200 years ago (0.2ka

1016 BP) and 6000 years ago (6ka BP estimated using REVEALS, and the difference in fractional cover
1017 between the two periods (0.2 ka BP - 6ka BP), where red indicates an increase in open land and blue
1018 a decrease (after Dawson et al., 2018).

1019
1020 Figure 8: Quantitative comparison of the change in climate between the mid-Holocene (6ka) and the
1021 pre-industrial period as shown by pollen-based reconstructions gridded to 2 x 2° resolution to be
1022 compatible with the model resolution (from Bartlein et al., 2011) and in simulations with and without
1023 the incorporation of land-use change (from Smith et al., 2016). This figure illustrates the approach
1024 that will be taken to evaluate the impact of new LULC scenarios on climate. The imposed land-use
1025 changes at 6000 years ago (6ka BP) were derived from the KK10 scenario (Kaplan et al., 2011). The
1026 plots show comparisons of mean annual temperature (MAT), mean temperature of the coldest month
1027 (MTCO) and mean annual precipitation (MAP) for the northern extratropics (north of 30° N), where
1028 each dot represents a model grid cell where comparisons with the pollen-based reconstructions is
1029 possible. Although the incorporation of land use produces somewhat warmer and wetter climates in
1030 these simulations, overall the incorporation of land-use produces no improvement of the simulated
1031 climates at sites with pollen-based reconstructions.

1032
1033 Figure 9: Illustration of the terrestrial C budget approach to evaluate LULC. The total terrestrial C
1034 balance (green circle 'total') is constrained by ice core records of CO₂ and its isotopic signature ($\delta^{13}\text{C}$).
1035 Estimates for C balance changes of different natural land carbon cycle components (e.g., peatlands,
1036 permafrost, forest expansion/retreat, desert greening) can be estimated independently (blue slices
1037 'Natural components') either from empirical upscaling of site-scale observations or from model-based
1038 analyses (BGC models forced with varying climate). The remainder (yellow slice 'remainder') is then
1039 calculated as the total terrestrial C balance (green circle 'total') minus the sum of separate estimates
1040 of natural components (blue slices 'Natural components') The remainder is effectively the emissions
1041 resulting from LULC changes, and can therefore be compared to LULC CO₂ emission estimates by
1042 carbon-cycle models.

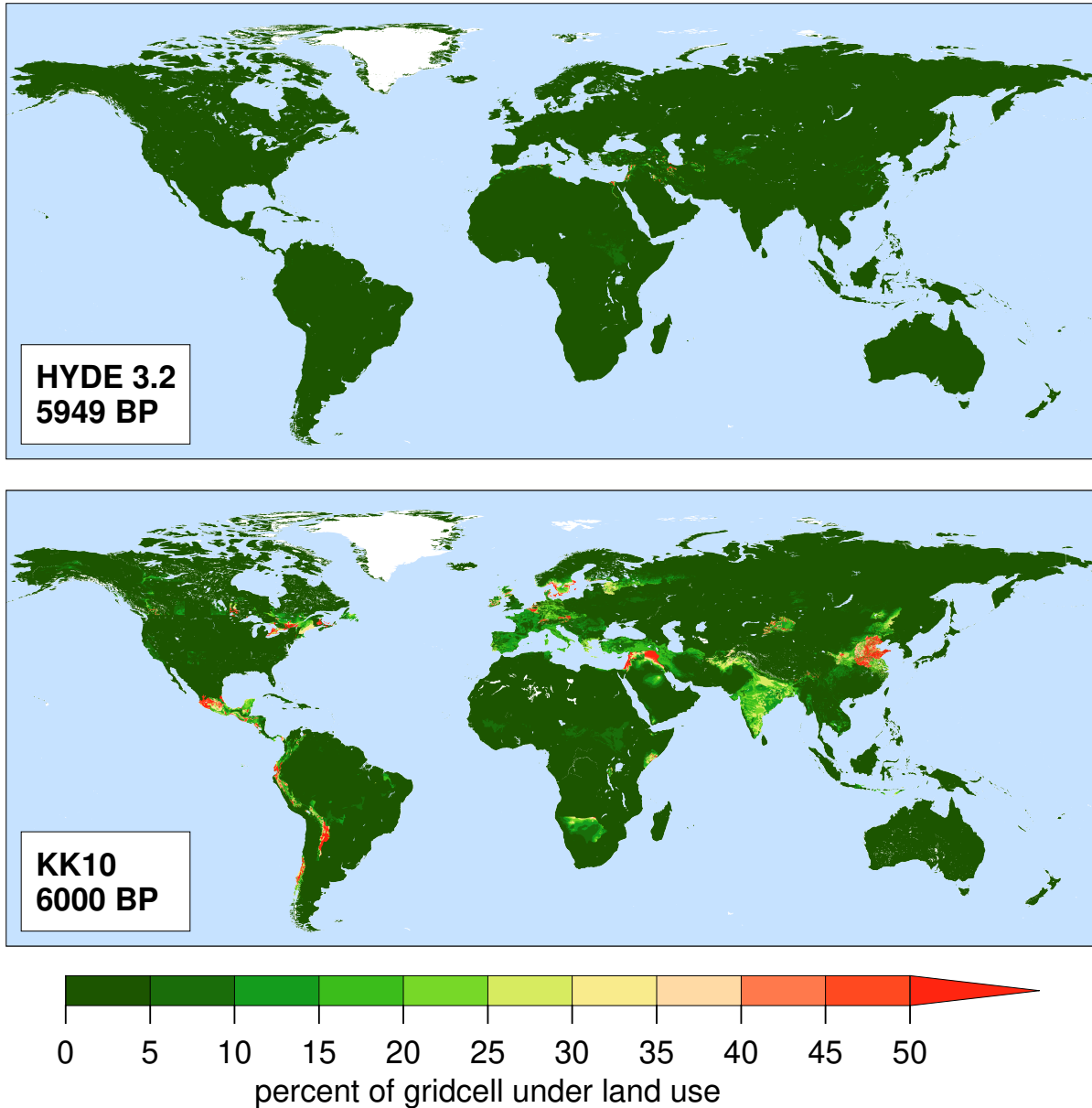
1043
1044 Table 1. Boundary conditions for CMIP6-PMIP4 and the mid-Holocene LULC experiments. The
1045 boundary conditions for the CMIP6-PMIP4 piControl and midHolocene are described in Otto-
1046 Bleisner et al. (2017) and are given here for completeness.

1047
1048 Table 2. Boundary conditions for baseline PMIP Holocene transient (6 ka BP to 1850 CE) and LULC
1049 transient simulations

1050
1051 Table 3. Summary of proposed simulations.

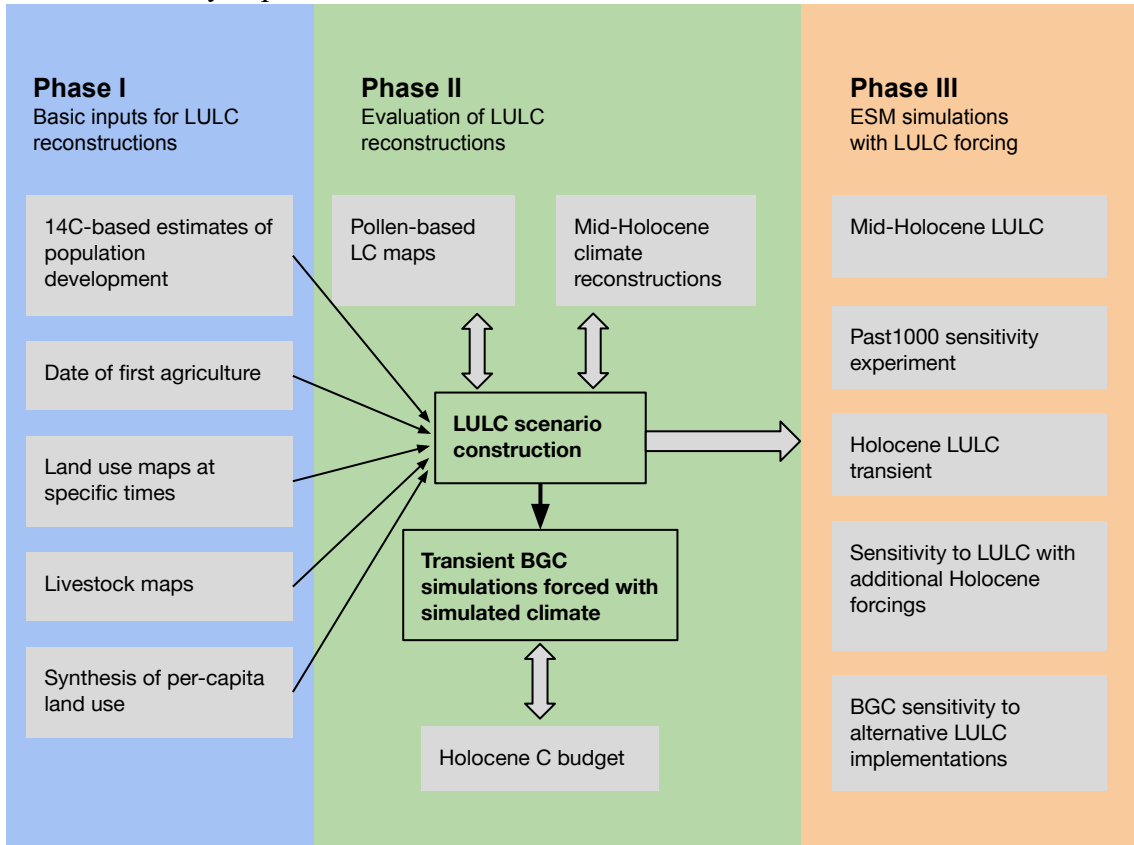
1052
1053

1054 Figure 1: Land use at ca 6000 years ago (6ka BP, 4000 years BCE) from the two widely used global
1055 historical land-use scenarios HYDE 3.2 (top panel, Klein Goldewijk et al. 2017a) and KK10 (bottom
1056 panel, Kaplan et al. 2011), illustrating the large disagreement between LULC scenarios at a regional
1057 scale. In both scenarios, the land-sea mask and lake areas are for the present day.
1058



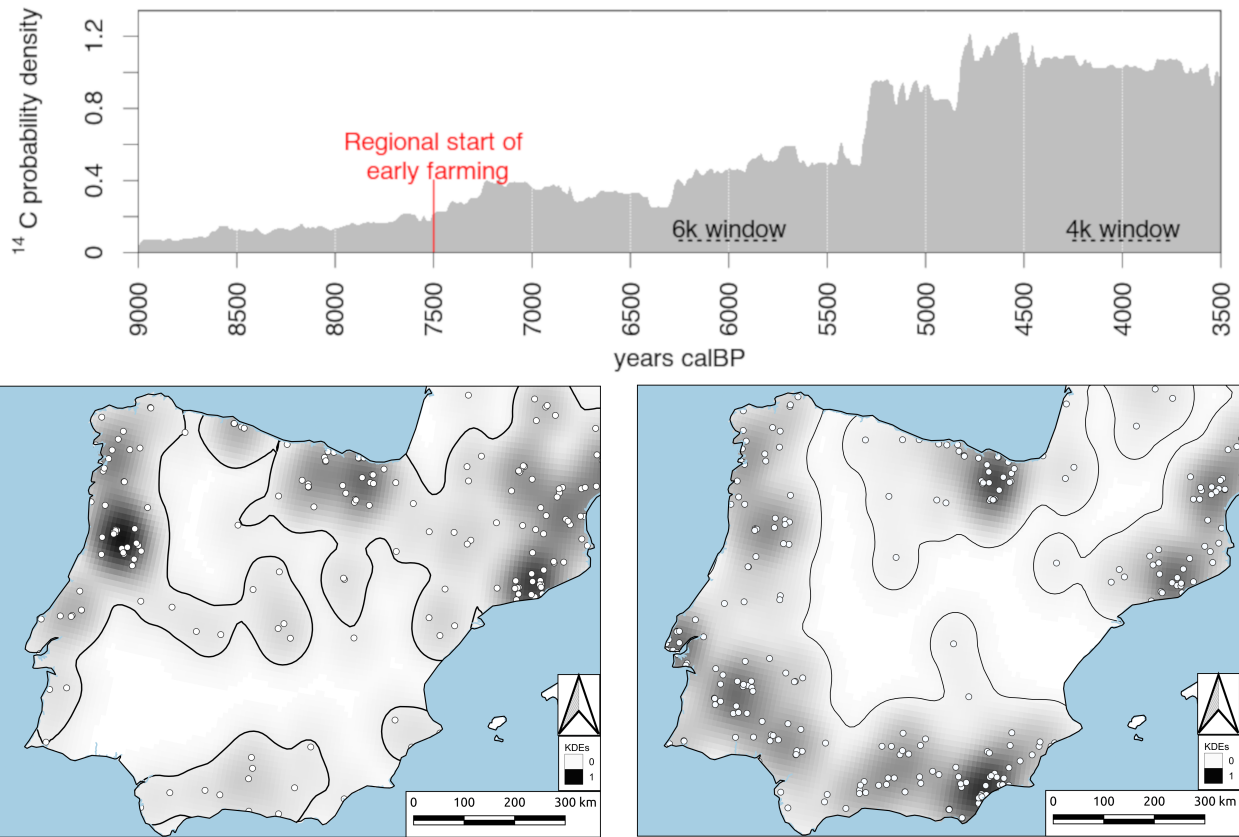
1059
1060

1061 Figure 2: Proposed scheme for developing robust LULC scenarios through iterative testing and
 1062 refinement, as input to Earth System Model (ESM) simulations. The archaeological inputs developed
 1063 in Phase 1 can be used independently or together to improve the LULC reconstructions; iterative
 1064 testing of the LULC scenario reconstruction (Phase 2) will ensure that these inputs are reliable before
 1065 they are used of ESM simulations (Phase 3). The uppermost three LULC simulations capitalize on
 1066 already planned baseline simulations without LULC; the lowermost two simulations are envisaged
 1067 as new sensitivity experiments.



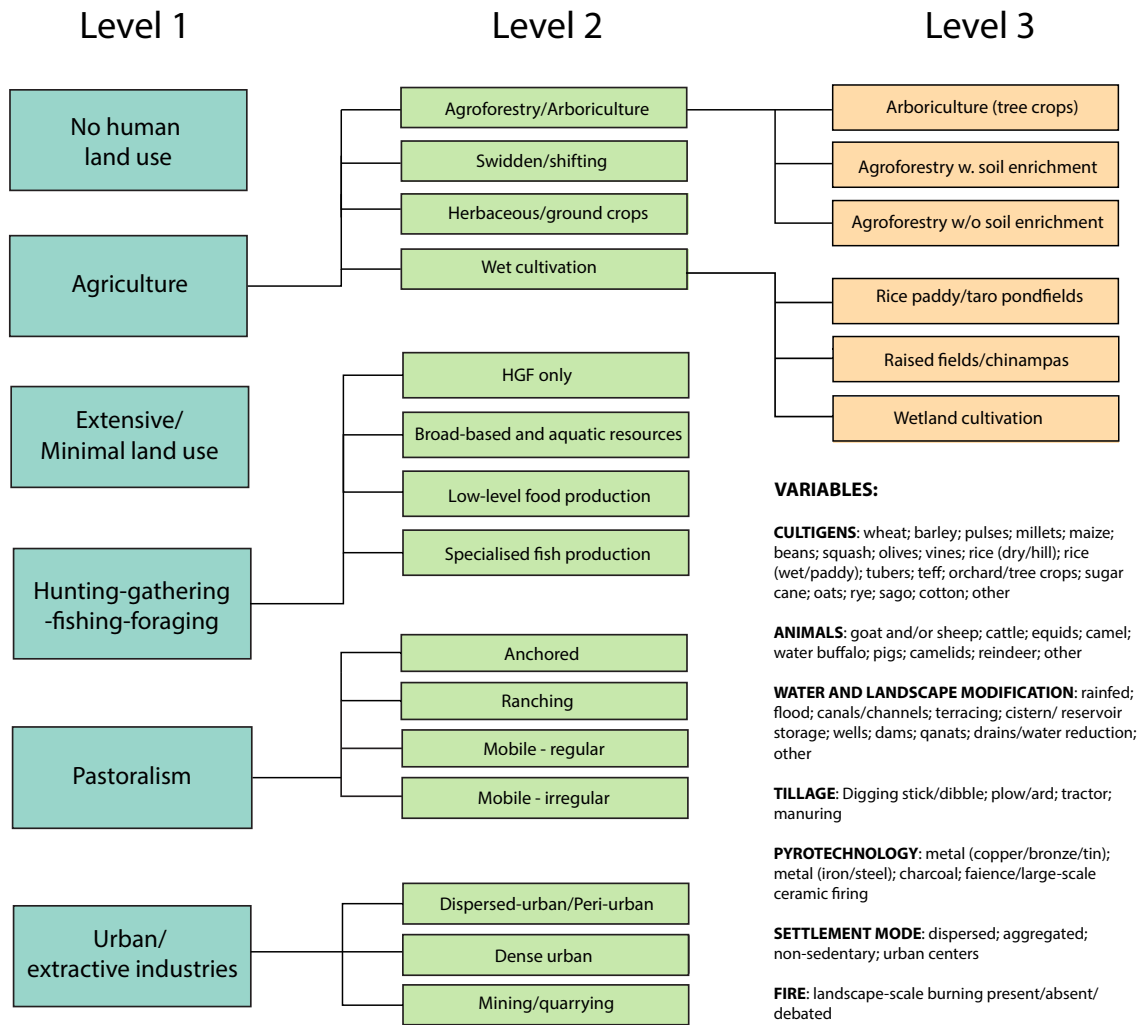
1068
1069

1070 Figure 3: Reconstruction of changes in population size in the Iberian Peninsula during the Holocene
1071 (9000 to 2000 BP, 9ka to 2ka BP) using summed probability distributions (SPDs) of radiocarbon
1072 dates (data after Balsera et al., 2015). The red line indicates the onset of agriculture in the region. The
1073 lower panels show areas under human use at 6ka (left) and 4ka (right) using kernel density estimates,
1074 where the white dots are actual archaeological sites and the shading shows the implied density of
1075 occupation.



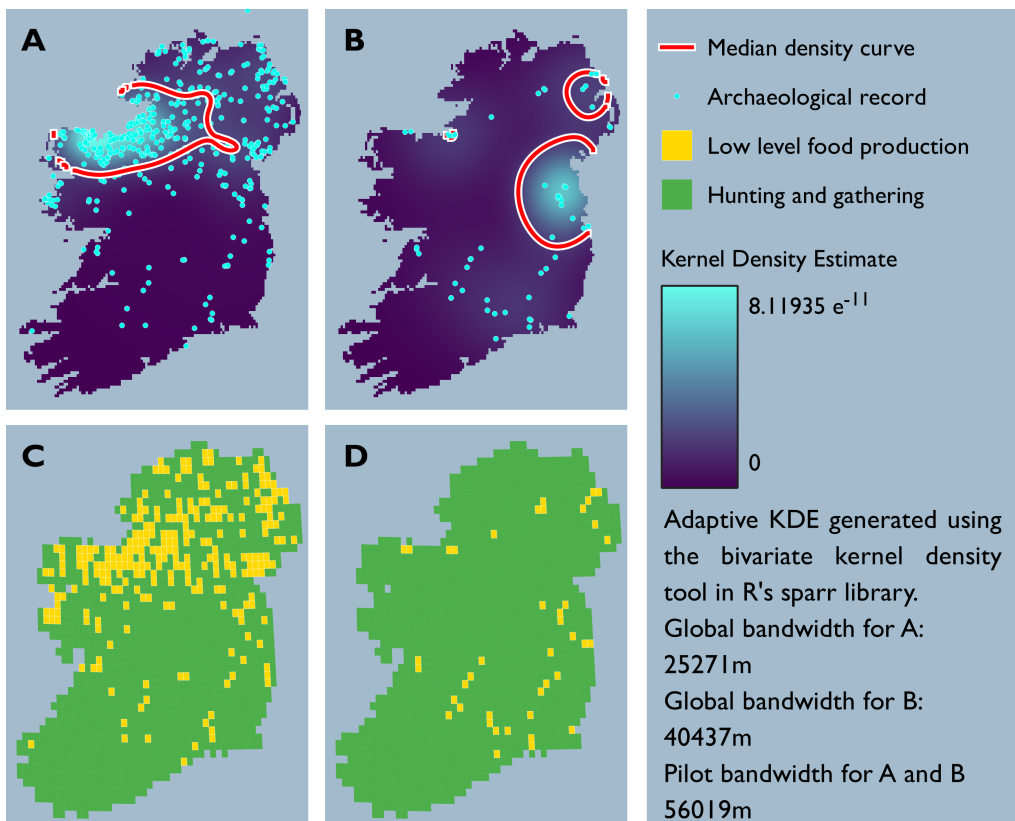
1076
1077

1078 Figure 4: The hierarchical scheme of land-use classes used for global mapping in LandCover6k
 1079 (updated from Morrison et al, 2018).



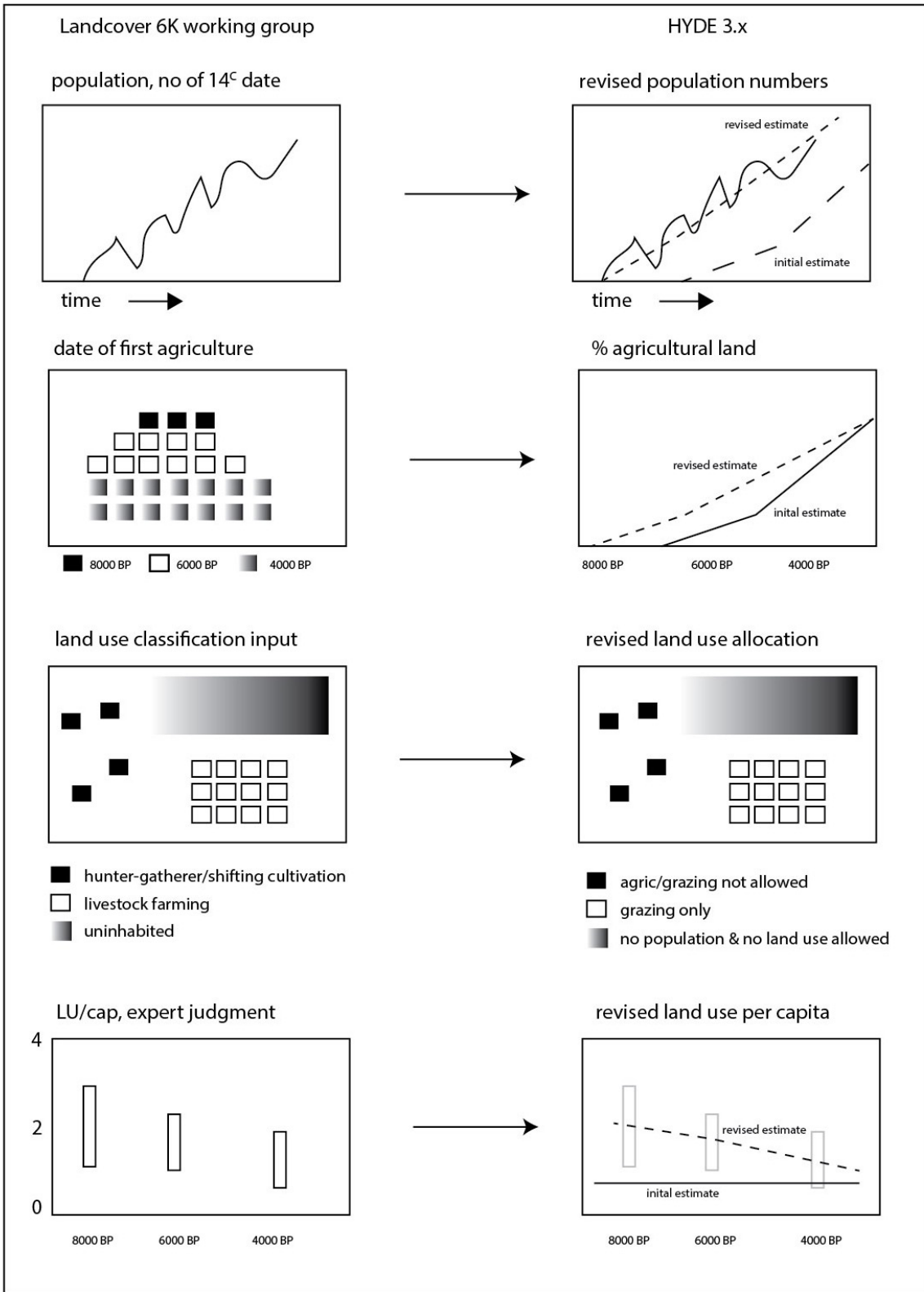
1080
 1081

1082 Figure 5: An example of regional land-use mapping. The upper panels show the distribution of known
 1083 archaeological sites superimposed on kernel density estimates of the extent of land-use based on the
 1084 density of observations, and the lower panels show these data superimposed on the LandCover6k
 1085 land-use classes for the Middle Neolithic (3600-3400 years BCE, 5600-5400 years BP, 5.6-5.4 ka
 1086 BP) (left panels) and the Early Neolithic (3750-3600 years BCE, 5750-5600 years BP, 5.7-5.6 ka BP)
 1087 (right panels) of Ireland. Data points derive from ¹⁴C dated archaeological sites and distributions of
 1088 settlements and monuments that have been assigned to each archaeological period following the
 1089 dataset published in McLaughlin et al. (2016). The assigned land-use classes are inferred from
 1090 archaeological material from one (or more) sites within the grid box. It should not be assumed that
 1091 the whole gridcell was being used for agriculture during the Middle and Early Neolithic. Informed
 1092 assessment suggests that agricultural land (crop growing and grazing, combined) probably occupied
 1093 between 10-15% of the total grid area in the low-level food production regions of the eastern and
 1094 western coastal areas, whilst agricultural land likely represents 5% or less of the total grid cell area
 1095 in inland areas.



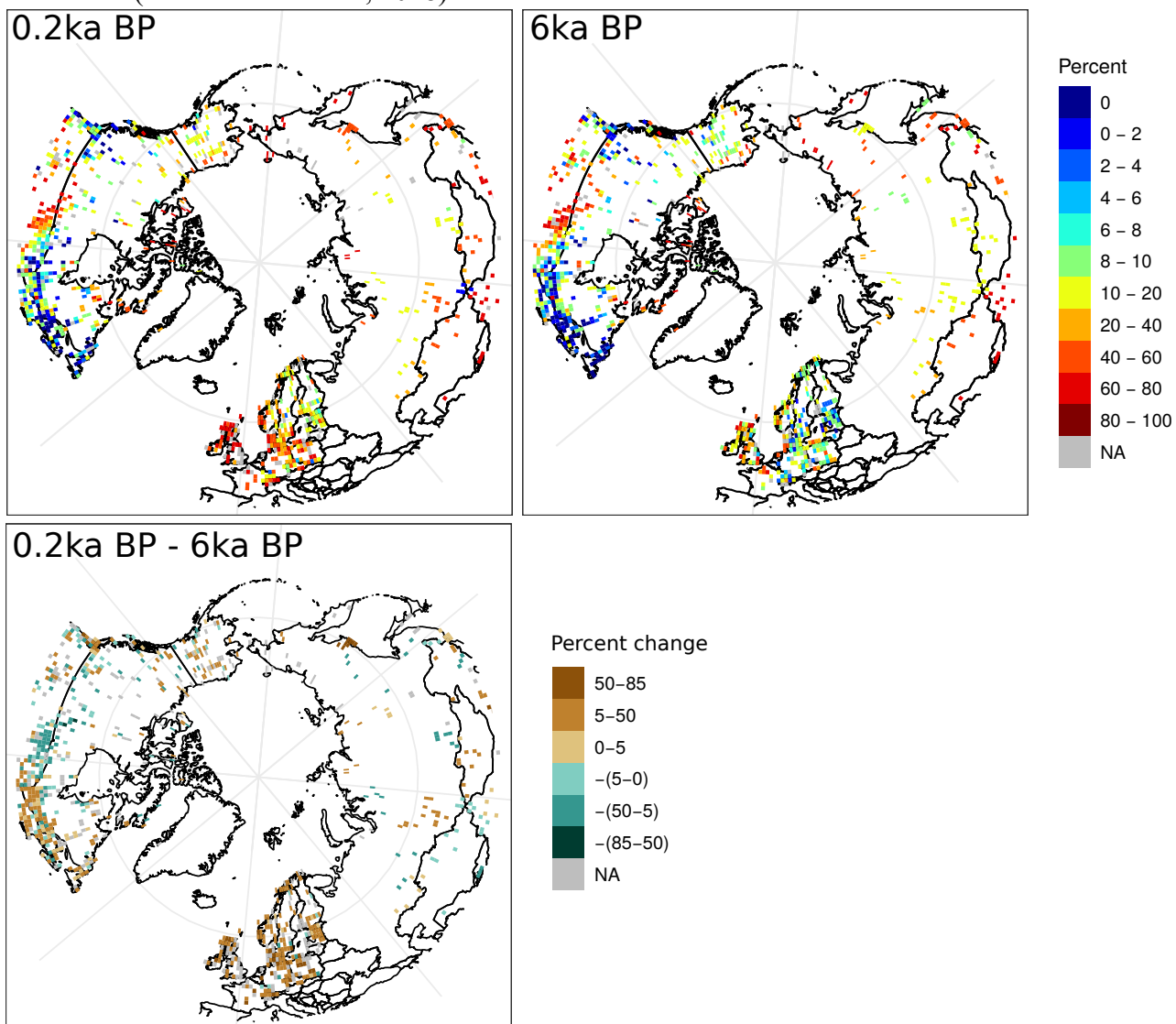
1096
 1097

1098 Figure 6: Schematic illustration of the proposed implementation of ^{14}C -based population estimates,
1099 date of first agriculture, land-use maps, and land-use per capita information in the HYDE model (here
1100 indicated as HYDE3.x). The archaeological data are represented as values for a grid cell in geographic
1101 space at a given time for date of first agriculture and land use, but as a time series for a specific grid
1102 cell for population and land-use per capita. In the case of population estimates, date of first agriculture
1103 and land-use per capita data, we show the initial estimate and the revised estimate after taking the
1104 archaeological information into account in the HYDE3.x plot. It should be assumed in the case of the
1105 land-use mapping that the original estimate was that there was no land use in this region.



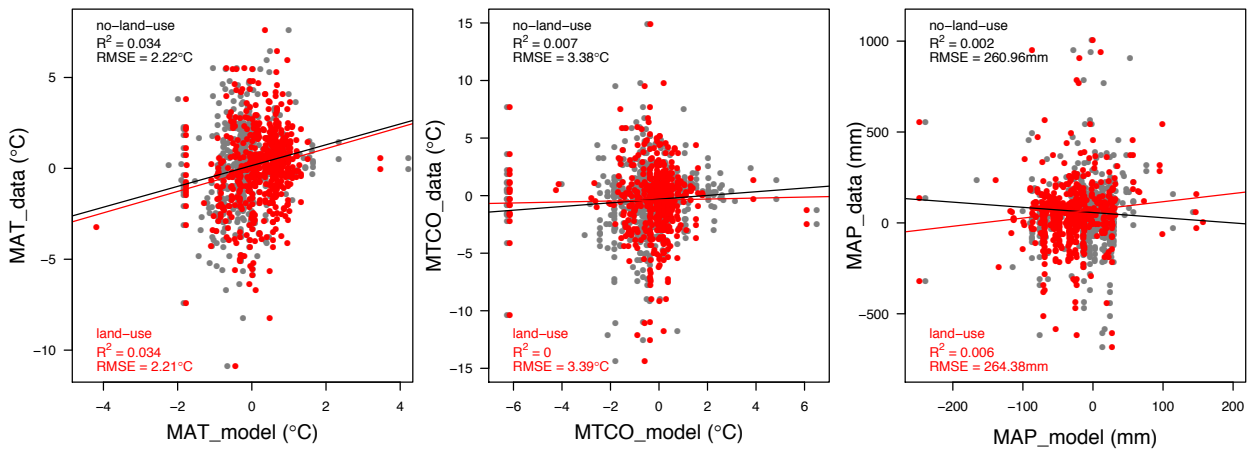
1106
1107

1108 Figure 7: Northern extratropical (>40°N) mean fractional cover of open land at 200 years ago (0.2ka
 1109 BP) and 6000 years ago (6ka BP estimated using REVEALS, and the difference in fractional cover
 1110 between the two periods (0.2 ka BP - 6ka BP), where red indicates an increase in open land and blue
 1111 a decrease (after Dawson et al., 2018).



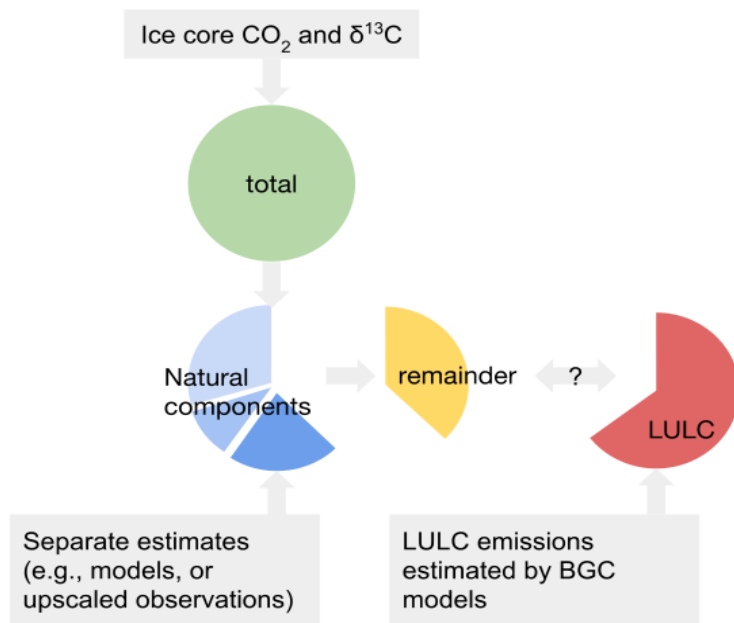
1112
 1113

1114 Figure 8: Quantitative comparison of the change in climate between the mid-Holocene (6ka) and the
1115 pre-industrial period as shown by pollen-based reconstructions gridded to 2 x 2° resolution to be
1116 compatible with the model resolution (from Bartlein et al., 2011) and in simulations with and without
1117 the incorporation of land-use change (from Smith et al., 2016). This figure illustrates the approach
1118 that will be taken to evaluate the impact of new LULC scenarios on climate. The imposed land-use
1119 changes at 6000 years ago (6ka BP) were derived from the KK10 scenario (Kaplan et al., 2011). The
1120 plots show comparisons of mean annual temperature (MAT), mean temperature of the coldest month
1121 (MTCO) and mean annual precipitation (MAP) for the northern extratropics (north of 30° N), where
1122 each dot represents a model grid cell where comparisons with the pollen-based reconstructions is
1123 possible. Although the incorporation of land use produces somewhat warmer and wetter climates in
1124 these simulations, overall the incorporation of land-use produces no improvement of the simulated
1125 climates at sites with pollen-based reconstructions.



1126
1127

1128 Figure 9: Illustration of the terrestrial C budget approach to evaluate LULC. The total terrestrial C
 1129 balance (green circle 'total') is constrained by ice core records of CO₂ and its isotopic signature (δ¹³C).
 1130 Estimates for C balance changes of different natural land carbon cycle components (e.g., peatlands,
 1131 permafrost, forest expansion/retreat, desert greening) can be estimated independently (blue slices
 1132 'Natural components') either from empirical upscaling of site-scale observations or from model-based
 1133 analyses (BGC models forced with varying climate). The remainder (yellow slice 'remainder') is then
 1134 calculated as the total terrestrial C balance (green circle 'total') minus the sum of separate estimates
 1135 of natural components (blue slices 'Natural components') The remainder is effectively the emissions
 1136 resulting from LULC changes, and can therefore be compared to LULC CO₂ emission estimates by
 1137 carbon-cycle models.
 1138



1139

1141
1142
1143
1144

Table 1. Boundary conditions for CMIP6-PMIP4 and the mid-Holocene LULC experiments. The boundary conditions for the CMIP6-PMIP4 *piControl* and *midHolocene* are described in Otto-Bleisner et al. (2017) and are given here for completeness.

Boundary conditions		1850CE (DECK <i>piControl</i>)	6ka (<i>midHolocene</i>)	6ka LULC (<i>midHoloceneLULC</i>)	
Orbital parameters	Eccentricity	0.016764	0.018682	0.018682	
	Obliquity	23.459	24.105	24.105	
	Perihelion – 180	100.33	0.87	0.87	
	Vernal equinox	Noon, 21 March	Noon, 21 March	Noon, 21 March	
Greenhouse gases	Carbon dioxide (ppm)	284.3	264.4	264.4	
	Methane (ppb)	808.2	597.0	597.0	
	Nitrous oxide (ppb)	273.0	262.0	262.0	
	Other GHG	DECK <i>piControl</i>	0	0	
Other boundary conditions	Solar constant	TSI: 1360.747	<i>As piControl</i>	<i>As piControl</i>	
	Palaeogeography	Modern	<i>As piControl</i>	<i>As piControl</i>	
	Ice sheets	Modern	<i>As piControl</i>	<i>As piControl</i>	
	Vegetation	Interactive	Interactive	Interactive	pasture and crop distribution prescribed from the revised scenario
		DECK <i>piControl</i>	<i>As piControl</i>	<i>As piControl</i>	pasture and crop distribution prescribed from the revised scenario
	Aerosols	interactive	Interactive	Interactive	Interactive
DECK <i>piControl</i>		<i>As piControl</i>	<i>As piControl</i>	<i>As piControl</i>	

1145
1146

1147 **Table 2.** Boundary conditions for baseline PMIP Holocene transient (6 ka BP to 1850 CE) and LULC
 1148 transient simulations

		Mode	Source/Value	LULC experiment
Orbital parameters		transient		As baseline simulation
Greenhouse gases	CO ₂	transient	Dome C	As baseline simulation
	CH ₄		Combined EPICA & GISP record	As baseline simulation
	N ₂ O		Combined EPICA NGRIP, & TALDICE record	As baseline simulation
Solar forcing		transient	Steinhilber et al. (2012)	As baseline simulation
Volcanic forcing		transient	To be determined	As baseline simulation
Palaeogeography		Constant at PI values	Modern	As baseline simulation
Ice sheets		Constant at PI values	Modern	As baseline simulation
Vegetation		interactive		LC6k transient pasture and crop distribution imposed
Aerosols		Constant at PI values		As baseline simulation

1149 **Table 3:** Summary of proposed simulations.
 1150

Name	Mode	Purpose
<i>piControl</i>	equilibrium	Standard CMIP6-PMIP4 simulation
<i>midHolocene</i>	equilibrium	Standard CMIP6-PMIP4 simulation
<i>midHoloceneLULC</i>	equilibrium	Sensitivity to LULC changes
<i>holotrans</i>	transient	Baseline fully transient simulation from 6ka onwards, with no LULC
<i>holotrans_LULC</i>	transient	Fully transient simulation from 6ka onwards, with LULC imposed

1151